Date of publication xxxx 00, 0000, date of current version xxxx 00, 0000.

Digital Object Identifier 10.1109/ACCESS.2017.Doi Number

A Comprehensive Survey on "Various Decoupling Mechanisms with Focus on Metamaterial and Metasurface Principles Applicable to SAR and MIMO Antenna Systems"

Mohammad Alibakhshikenari[1], *Member IEEE,* Fatemeh Babaeian[2], *Member IEEE,* Bal S. Virdee[3], *Senior Member IEEE*, Sonia Aïssa[4], *Fellow IEEE*, Leyre Azpilicueta[5], *Senior Member IEEE*, Chan H. See[6], *Senior Member IEEE,* Ayman Abdulhadi Althuwayb[7], *Member IEEE*, Isabelle Huynen[8], *Senior Member IEEE*, Raed Abd-Alhameed[9], *Senior Member IEEE,* Francisco Falcone[10,11], *Senior Member IEEE*, and Ernesto Limiti[1], *Senior Member IEEE*

[1] Electronic Engineering Department, University of Rome "Tor Vergata", Via del Politecnico 1, 00133 RM, Rome, Italy

[2] Department of Electrical and Computer Systems Engineering, Monash University, Melbourne, Australia

[3] London Metropolitan University, Center for Communications Technology, London N7 8DB, UK

[4] Institut National de la Recherche Scientifique (INRS), University of Quebec, Montreal, QC, H5A 1K6, Canada

[5] School of Engineering and Sciences, Tecnologico de Monterrey, Monterrey 64849, Mexico

[6] School of Engineering & the Built Environment, Edinburgh Napier University, 10 Colinton Rd., Edinburgh, EH10 5DT, UK

[7] Electrical Engineering Department, Jouf University, Sakaka, Aljouf 72388, Kingdom of Saudi Arabia

[8] Institute of Information and Communication Technologies, Electronics and Applied Mathematics, Université Catholique de Louvain, 1348 Louvain-la-Neuve , Belgium

[9] Faculty of Engineering and Informatics, University of Bradford, Bradford, West Yorkshire, BD7 1DP, UK

[10] Electric, Electronic and Communication Engineering Department, Public University of Navarre, 31006 Pamplona, Spain

[11] Institute of Smart Cities, Public University of Navarre, 31006 Pamplona, Spain

Corresponding author: Dr. Mohammad Alibakhshikenari (alibakhshikenari@ing.uniroma2.it)

ABSTRACT Nowadays synthetic aperture radar (SAR) and multiple-input-multiple-output (MIMO) antenna systems with the capability to radiate waves in more than one pattern and polarization are playing a key role in modern telecommunication and radar systems. This is possible with the use of antenna arrays as they offer advantages of high gain and beamforming capability, which can be utilized for controlling radiation pattern for electromagnetic (EM) interference immunity in wireless systems. However, with the growing demand for compact array antennas, the physical footprint of the arrays needs to be smaller and the consequent of this is severe degradation in the performance of the array resulting from strong mutual-coupling and crosstalk effects between adjacent radiating elements. This review presents a detailed systematic and theoretical study of various mutual-coupling suppression (decoupling) techniques with a strong focus on metamaterial (MTM) and metasurface (MTS) approaches. While the performance of systems employing antenna arrays can be enhanced by calibrating out the interferences digitally, however it is more efficient to apply decoupling techniques at the antenna itself. Previously various simple and cost-effective approaches have been demonstrated to effectively suppress unwanted mutual-coupling in arrays. Such techniques include the use of defected ground structure (DGS), parasitic or slot element, dielectric resonator antenna (DRA), complementary split-ring resonators (CSRR), decoupling networks, P.I.N or varactor diodes, electromagnetic bandgap (EBG) structures, etc. In this review, it is shown that the mutual-coupling reduction methods inspired by MTM and MTS concepts can provide a higher level of isolation between neighbouring radiating elements using easily realizable and cost-effective decoupling configurations that have negligible consequence on the array's characteristics such as bandwidth, gain and radiation efficiency, and physical footprint.

INDEX TERMS Decoupling methods, metamaterial (MTM), metasurface (MTS), multiple-input-multiple-output (MIMO), synthetic aperture radar (SAR), isolation enhancement, array antennas.

I. INTRODUCTION

SAR and MIMO [1] are arguably the state-of-the-art methodologies for enhancing the capacity of radio links via multiple transmitting and receiving antennas to have multipath scattering. Conventionally, MIMO and SAR

systems are defined as practical techniques for transmitting and receiving signals stemming from multiple independent channels concurrently. This is typically implemented over the same radio channel with the aid of multiple antenna configurations without additional losses in radiation power in rich scattering surroundings. SAR and MIMO are also categorized under next generation wireless communication technologies due to their marked potential to improve system credibility and channel capacity by means of multiple antennas [2]. MIMO was as a practical solution to the data rate restriction of single-input single-output (SISO) systems. MIMO and SAR are generally used on different networks, and they also improve the transmission velocity of data [3] by using the maximum content of wireless telecommunication devices.

In [4-5], various etched portable MIMO and SAR antenna apparatus are discussed. They are broadly applied in applications of mobile devices because of their adaptation with the system, better completeness, low cost, and simplicity of construction. The simplicity and genericity of the multi-antenna topology [6] utilized in the transmitting side and receiving side in MIMO and SAR systems allow for a more convenient implementation compared to other antenna array topologies. Also, such configurations reduce channel errors in communication systems to have enhanced data rates [7]. However, this may lead to multipath scattering due to the inherent high cohesion factor in the multi-signal distribution [8]. Additionally, the decreased distance between the antennas in array systems can potentially reduce the decoupling factor, which degrades the angle of arrival [9] in the estimation of carrier frequency offset [10] and signal to interference noise ratio [11]. It is good to note that the isolation between adjacent antennas decreases either by a huge flow of surface current from the stimulated ports or space radiation and surface waves. Also, the contrary influence of interferences on reflection coefficients cannot be ignored [12]. Hence, the main challenge in the implementation of antennas for MIMO and SAR applications is limiting the interferences between more recent compact etched antennas and other antenna configurations [13], [14]. Comprehensive studies based on models specifically designed to increase the isolation have been presented in recent times [15-27]. The basic approaches for enhancing isolation in multi-antenna systems typically involve the utilize of decoupling networks [17], neutralization lines [18-20], engraved parasitic elements [21], CSRRs [22], EBG architectures [23], DGSs [24, 25], and metasurfaces (MTS) and metamaterials (MTM) [26, 27]. Besides the multi-antenna systems, the decoupling methods to increase the isolation in broadband base station arrays have been presented in [28], [29]. In [30], easy comparison of disparate decoupling approaches containing parasitic elements, utilize PIN and varactor diodes, and decoupling networks has provided. In addition, the efficacy of varying relative permittivity of layers on antenna parameters is presented and discussed. These methods allow for the manipulation of mutual coupling through weakening, resisting, or reducing the surface current flow. Antenna configurations such as reconfigurable, engraved, dielectric resonator, metasurface, and metamaterial are widely adopted to destroy the harmful outcome of the interferences [30-35].

In the following survey, a comparative review is given on diverse methodologies for suppressing mutual-coupling in antenna arrays for application in MIMO and SAR systems based on metasurface (MTS) and metamaterial (MTM) properties. In addition, different antenna models based on conventional decoupling techniques are examined. The antenna performance is characterised in terms of operating frequency range, degree of isolation between adjacent radiators, radiation gain and efficiency. In essence, this survey highlights the practicality and constraints of various mutual-coupling suppression techniques for antenna arrays that are available today to antenna designers. Though in [30], [36-37] the theoretical aspects of SAR and MIMO antenna isolation are discussed, these articles do not discuss the diverse range of mutual-coupling isolation. Moreover, there is a dearth of literature on the current techniques and design principles for mitigating mutual coupling in antenna arrays based on the MTS and MTM properties. This survey provides the latest diverse decoupling techniques available to improve their radiation performance of high dense antenna arrays.

Rest of the paper has organized as follows. Section II is on mutual coupling definition. Section III is on the various decoupling methods. Sections IV and V present the main parts of this survey which focus on the diverse decoupling methods inspired metamaterials and metasurfaces for antenna array application in MIMO and SAR systems. Section V also provides a comprehensive comparison table which includes several research studies. Finally, this survey has concluded in Section VI.

II. MUTUAL COUPLING DEFINITION

In antenna array systems, the mutual coupling generally refers to the energy attracted through a nearby antenna when an antenna is operational. It changes the reflection coefficient(s), input impedance(s), and radiation pattern(s). To provide an analytical background for mutual coupling, some empirical models have been presented and discussed in [38], according to Equation (1) and Equation (2).

$$MC_{mn} = \exp(-\frac{2.d_{mn}}{\lambda}(\alpha + j\pi)), \quad m \neq n \qquad (1)$$

$$MC_{mm} = 1 - \frac{1}{N}\sum_m \sum_{m \neq n} MC_{mn} \qquad (2)$$

where MC_{mn} represents the mutual coupling and the space between the m^{th} and n^{th} antennas is defined by d_{mn}. The number of antennas and the parameter controlling the level of coupling are presented by N and α, respectively.

Practically, the isolation level pertains not only to the array topology but also on the stimulations of the array antennas and other factors. It is normally estimated applying the dB-valued S-parameter between the m^{th} and n^{th} antennas (i.e., $20 \log 10\ (|S_{mn}|)$), and equivalently the isolation $-20 \log 10\ (|S_{mn}|)$ between them.

A detailed understanding of the isolation mechanism will invariably relate to the transmitting/receiving mode. The isolation mechanisms are discussed below, considering the transmitting and receiving modes independently.

A. ISOLATION IN TRANSMITTING MODE

Fig.1 displays that the antennas *"m"* and "*n"* in a typical array are considered. A generator is considered to antenna *"n"*, the produced energy of the generator "1" radiates within area "2" and onto the m^{th} antenna "3". The portion of the energy arrived at the m^{th} antenna re-scatters within area "4" and the residual energy moves in the direction of the source "5". A deduction of the re-scattered energy "4" will be take-up by the n^{th} antenna "6". This mutual interplay is an ongoing procedure, and it is iterative. However, it is usually best to select the first few repetitions because the re-scattered energy reduces drastically after each repetition. The general far-field is derived from the vector summation of the re-scattered and radiated fields. Hence, the mutual coupling varies the pattern of the antenna. The wave "5" is added vectorially to the reflected wave and incident wave of the m^{th} antenna. This enhances the standing wave and changes the m^{th} antenna's input impedance. Mutual coupling varies both the self-impedance of the antenna and the mutual impedance.

B. ISOLATION IN RECEIVING MODE

Assuming the plane wave "1" exceed toward the array reaching the m^{th} antenna. It evolves a current in the m^{th} antenna. The portion of the incident wave travels within the receiver as "2" and the remaining segment is re-scattered within area "3". Some of the re-scattered wave is conducted onto the n^{th} antenna "4", where it adds (vectorially) to the incident plane wave "5". Thus, the received wave through an element is the vector summation of the direct waves and the coupled waves from other elements. To optimize the received energy (i.e., lowest re-scattered energy), the m^{th} antenna's terminating impedance has to be selected. Therefore, the re-scattered wave "3" is annulled via the reflected wave "5". In a receiving mode, the antenna's performance under consideration can be evaluated through stimulating the antenna with the other antenna interrupted with a 50-ohm load.

III. VARIOUS DECOUPLING TECHNIQUES

In literature, several isolation enhancement approaches are available such as decoupling networks, parasitic element approach, slot etching and ground plane structures, neutralization lines, PIN diode, varactor diode and feeding structures, frequency-selective surface (FSS), characteristic modes, and EBG structures [13-14], [15-16], [30], [35-37]. These approaches have been briefly discussed in this section. Additionally, due to some disadvantages and restrictions of the abovementioned methods, which have been discussed in details in the next part, the metasurface and metamaterial decoupling methods have been proposed and investigated in deep, which enable the designers to model SAR and MIMO antenna systems with minimized mutual coupling in a compact footprint area for mass production.

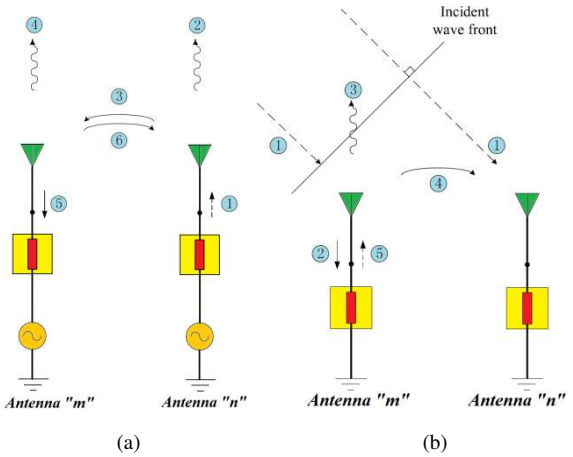

Fig.1. Investigation of mutual coupling architecture in (a) transmitting and (b) receiving modes [14].

A. DECOUPLING NETWORK APPROACH

Decoupling networks are applied to obtain enough isolation in MIMO and SAR antenna systems. They work on the methodology of the transformation of the cross-admittance term to purely imaginary amount via step up transmission lines or through discrete elements. Eigen mode disintegration [39], manmade structure [40], coupled resonator [41], and inserted elements [42] are some examples of the isolating layouts.

Modeling the decoupling scheme between the antenna arrays is easy to implement [35-52]. Specified decoupling approaches provide mutual reduction at the cost of some ohmic losses. The isolating method annuls the original interference by producing a supplementary coupling route; therefore, the mutual coupling is reduced, and far-field properties become better.

Similarly, the SAR and MIMO decoupling performance can be boosted through implementing an indistinct line and lumped components [53-55]. It is placed between the SAR and MIMO antenna arrays to increase gain and reduce the mutual coupling. The shunt component based decoupling network is applied to increment the performances to have acceptable decoupling between the antennas.

Various types of the decoupling network approaches to increment the decoupling between the array antennas have been presented and explained in the literature such as diamond-shaped patterned ground resonator (DSPGR)-plane decoupling network [56], dummy load-based decoupling approaches [57], coupled resonator decoupling network (CRDN) [58], and multi-element pattern diversity based decoupling network [59]. Table I depicts a comparison of the characteristics of MIMO antennas using decoupling networks. In [59], the highest efficiency and the lowest mutual coupling of -32 dB are achieved utilizing the most straightforward configuration of dummy loads. The dual-band operations are exhibited in [58].

TABLE I. COMPARISON ON THE PERFORMANCE PARAMETERS OF DECOUPLING NETWORKS BASED MIMO AND SAR ANTENNAS

Ref.	[56]	[57]	[58]	[59]
Dimensions / Substrate	72.4 × 20 × 0.8 mm^3 Rogers RO4350B	70 × 35 × 0.8 mm^3 FR-4	112 × 55 × 1.6 mm^3 FR-4	40 ×100 × 0.8 mm^3 FR-4
Isolation (dB)	≥ -27.6 dB @ 2.18 ~2.65 GHz	≥ -32 dB @ 3.45 ~3.55 GHz	≥ -15 dB @ 2.4 ~2.48 GHz ≥ -15 dB @ 5.15 ~5.35 GHz	≥ -15 dB @ 3.5 ~3.6 GHz
Applied Approach	Diamond-shaped pattern ground resonator	Reactive dummy loads	Coupled resonator decoupling method	Pattern diversity decoupling method
Efficiency / Gain	66~70.5 % / 1.39dBi	82 % / -	66~75 % / -	50% / -
No. of Ports / Applications	Dual Ports / IMS	Triple Ports / WiMAX	Dual Ports / ISM and WLAN	Eight Ports / WiMAX
Remarks	Complex layout and medium dimension	Easy configuration	Dual-band and Large dimension	Easy configuration and maximum ports

B. PARASITIC ELEMENT DECOUPLING APPROACH

Engraved slit or parasitic element antennas use two orthogonal modes to generate a broad frequency band via coupling in ground plane and/or in radiating patch [60]. In this method, the isolation between elements is optimized by producing an additional coupling route [61-62]. One of the two coupling routes opposes the signal arriving from the other coupling road, which causes an improvement in isolation level. Indirectly linked decoupling components such as folded shorting strip, meandered slot, and vertical parasitic strip are recognized as a parasitic element [63-65]. Ease of implementation, size, and comfortable generation applying PCB technology and/or waveguides are the main benefits of the parasitic or slot antenna. The placement of parasitic elements has to be implemented meticulously, and it is not very straightforward. This procedure increases the performance parameters of the array antennas.

Various types of the parasitic element decoupling approaches based on the square ring slit [66], metal strip reflector [67-68], stepped feed-line and open-ended ground slit [69], and single-shared-radiation component and meandered feeding lines [70] to obtain lowest interference between the array elements have been proposed and illustrated in the literature. Table II mentions the studied specifications of parasitic or slot antennas. The maximum amount of gain and bandwidth is achieved in [66]. The structure in [67] provides optimum efficiency with an easy layout. The antenna in [68] presents the highest isolation value of -22dB. A new shared radiation element antenna is investigated in [70].

TABLE II. COMPARISON ON THE PERFORMANCE PARAMETERS OF SLIT OR PARASITIC ELEMENT BASED MIMO AND SAR ANTENNAS

Ref.	[66]	[67]	[69]	[70]
Dimensions / Material	66.25 × 66.25 ×1.6 mm^3 FR-4	25 × 30 × 1.6 mm^3 FR-4	42 × 25 × 1.6 mm^3 FR-4	22 × 24.3 × 1.52 mm^3 Rogers TMM4
Isolation Level (dB)	≥ -20 dB @3.0 ~12.0 GHz	≥ -20 dB @3.1 ~10.6 GHz	≥ -22 dB @3.2 ~12.0 GHz	≥ -15 dB @3.0 ~10.6 GHz
Applied Approach	Square ring slot and stepped feed line	Two coplanar stripline-feed staircase-shaped radiating elements	Open-ended ground slot and stepped-slot feed line	Meandered feed line and stub to ground linked through via
Efficiency / Gain	60% / 5~8 dBi	90% / 5.2dBi	≤80% / 4dBi	82% / 1.5~5.8 dBi
No. of Ports / Applications	Dual Ports / UWB	Dual Ports / UWB	Quad Ports / Portable UWB	Dual Ports / UWB portable devices
Remarks	Lowest ECC	Simple manufacture and small dimension	Low mutual coupling	Maximum gain and expensive substrate

C. DEFECTED GROUND STRUCTURE (DGS) DECOUPLING METHOD

DGS introduces the slits realized on the antenna's ground plane [71]. It is pursued as an appearing method for improving many parameters of MIMO and SAR antenna systems [72]. Also, it participates dramatically to increment the isolation. A general way is to create the slit in the ground plane. Howbeit, the slit can improve the isolation, it may also enhance the back radiation [73-75]. Various sorts of slits can be engraved on the ground (GND) as well as on the patch for decoupling improvement, shifting frequency, footprint area decrement, and multiband operation. The printed slit controls the flowing current flowing on the ground plane by repressing the interferences between the adjacent elements and behaves such a band-stop filter.

Various types of the DGS isolating mechanisms have been discussed in the literature. A few examples of the these isolating mechanisms are S-shaped DGS [76], square ring DGS [77], T-shaped metallic stub based DGS [78], electrically small meandered DGS [24], [79], ground plane loaded with complementary split ring resonator (CSRR) [22], concentric square ring patch with CSRR loaded GND [80], CSRR loaded GND [81], and slotted CSRR in GND [82]. Properties of several DGS antennas

presented here are listed in Table III. This table explains that antenna in [76] has the largest size and thickness. The antenna in [76] also achieves the highest efficiency and isolation of -55 dB. Even though the antenna in [24] presents the largest bandwidth accompanying band notch property and small size, it depicts considerably higher isolation performance than [66].

TABLE III. COMPARISON ON THE PERFORMANCE PARAMETERS OF DGS MIMO AND SAR ANTENNAS

Ref.	[66]	[83]	[78]	[24]
Dimensions / substrate	100 × 72 × 3.81 mm^3 Rogers TMM6	60.2 × 60.2 × 1.6 mm^3 RF-4	22 × 26 × 0.8 mm^3 RF-4	50 × 160 × 0.8 mm^3 RF-4
Isolation Level (dB)	≥ -55 dB @ 2.57 GHz	≥ -25 dB @ 2.45 GHz	≥ -20 dB @ 3.1~11.8 GHz	≥ -20 dB @ 0.7~1.0 GHz
Applied Approach	S-formed periodic DGS	Square ring DGS	Trident-shaped Strip and Ground plane open ended slit	Open ended DGS-slit
Efficiency / Gain	93~96% / -1.79~3.75dBi	81% / 2.1dBi	85% / 3.6~6dBi	80% / 2dBi
No. of Ports/ Applications	Quad Ports/ WLAN	Quad Ports/ WLAN	Dual Ports/ UWB, WLAN, X-band notched	Quad Ports/ LTE
Remarks	Large thickness and high efficiency	Miniature structure and simple construction	Miniature structure and large bandwidth and filter	Complex structure and controllable isolation

Table IV shows the characteristics of the CSRR loaded ground plane antennas. For the antenna in [82], the highest efficiency at 86.62% and the most straightforward configuration with dual band properties is obtained. The antenna in [82] has higher isolation of -33 dB. Hence, it is more appropriate in comparison to other CSRRs.

TABLE IV. COMPARISON ON THE PERFORMANCE PARAMETERS OF CSRR MIMO AND SAR ANTENNA

Ref.	[22]	[80]	[81]	[82]
Dimensions / substrate	23 × 29 × 1.524 mm^3 Rogers TMM4	60 × 60 × 1.6 mm^3 FR-4	100 × 50 × 0.8 mm^3 FR-4	70 × 100 × 1.6 mm^3 Rogers4003
Isolation Level (dB)	≥ -15 dB @ 3 ~12 GHz	≥ -22 dB @ 2.2 ~2.7 GHz	≥ -18 dB @ 2.4~2.5 GHz	≥ -20 dB @2.45 GHz & ≥ -33 dB @5 GHz
Applied Approach	Stub and GND SCRR and	GND CSRR and concentric square ring patch and	GND and bottom plane CSRR	Slotted CSRR in GND
Efficiency / Gain	82% / 5.9dBi	72.57% / 4dBi	29% / -0.8dBi	86.64% / 4.025dBi
No. of Ports/ Applications	Dual Ports/ UWB	Quad Ports/ ISM	Quad Ports/ ISM	Dual Ports/ WLAN
Remarks	Large bandwidth and small structure	Horizontal and vertical polarized, easy layout	Large size and thinner thickness	Lowest mutual coupling, dual-band, and easy layout

D. NEUTRALIZATION LINE DECOUPLING APPROACH

Neutralization lines [84] are utilized to transit electromagnetic waves from one antenna to another via a metallic slot or lumped component. They create a contrary coupling which lowers the interferences at given frequencies between the elements. Neutralization lines have considered as particular isolation approaches, which annul the interferences via presenting a second road with an inverse phase and equal amplitude. Consequently, the utmost of neutralization lines accessible in literature are narrowband [85], [86]. The neutralization line is more appropriate for the SAR and MIMO systems with a low number of antenna arrays. In MIMO and SAR antenna models, the difficulty of matching is quite evident. A neutralization line is a metallic structure with a thin thickness that dissolves the obstacle of matching and suppresses the coupling between antennas. The form, dimensions, and orientation of the neutralization line are related to the antenna components. However, finding the neutralization path is not very straightforward.

Various implementations of the neutralization line decoupling approach to reduce the array antenna's mutual coupling such as thin printed neutralization lines [87], pair of crossed neutralization lines [88], neutralization lines together with LC matching network [18], and neutralization lines between ground planes [89] have been presented and investigated in the literature. Table V describes the neutralization-based MIMO and SAR antenna properties. A couple of crossed neutralization lines is investigated in [88] with the thinnest substrate thickness and proper gain amounts. However, the antenna's layout is not simple. The antenna operates on multiple frequency bands and presents a minimum mutual coupling amount of -23 dB.

TABLE V. COMPARISON ON THE PERFORMANCE PARAMETERS OF NEUTRALIZATION LINES MIMO AND SAR ANTENNAS

Ref.	[87]	[88]	[18]	[89]
Dimensions / Material	36 × 65 × 1 mm^3 FR-4	135 × 80 × 0.8 mm^3 FR-4	50 × 40 × 1.6 mm^3 FR-4	4 cm × 4 cm × 1.6 mm FR-4
Isolation Level (dB)	≥ -15 dB @ 2.4 ~2.5 GHz	≥ -23 dB @ 750, 850, 2000, 2500 MHz	≥ -20 dB @ 2.45 and 5.8 GHz	≥ -21 dB @ 3.1 ~11 GHz
Applied Approach	Neutralization line	Crossed neutralization line with integrated inductors	Neutralization line with couple of inductor and capacitor	Stepped neutralization line
Efficiency / Gain	81% / 2.1dBi	31.86~61.73% / -1.79~3.75 dBi	78~85% / -	- / 3.28~4dBi
No. of Ports / Applications	Dual Ports / WLAL USB-Dongle	Dual Ports / LTE, GSM, WLAN	Dual Ports / WLAN	Quad Ports / UWB
Remarks	Small structure and easy configuration	Complex layout and minimum isolation	high efficiency and easy layout	Large dimension, largest bandwidth, and simple configuration

E. PIN DIODE, VARACTOR DIODE, AND FEEDING STRUCTURE DECOUPLING APPROACH

PIN diode, varactor diode, and feeding structures are also applied to suppress the mutual coupling effects [90]. PIN diode in antenna models generates dynamic radiation patterns. The implementation of PIN diode in MIMO and SAR antenna arrays results to enlarge the link capacity controls the antenna's length, and also increments decoupling. This attribute ensures the reconfigurability of the antenna's radiation [91].

Several switching-based decoupling methods where MEMS switches, *p-i-n* and varactor diodes are applied to expand the working frequency band and degrade the coupling have been proposed in the literature [92]. Some of them are based on back-to-back MEMS switches [93], slot-based P-I-N diodes [94, 95], planar inverted-F P-I-N diodes [96], and microstrip loop and slit frequency reconfigurable [97]. Table VI lists the characteristics of the mentioned approaches. The antenna illustrated in [96] is not simple because of the presence of a shorting plate and a vertical corrected feed line. It has the maximum amount of gain. Also, it has the highest isolation amount of -47 dB. However, the antenna structure in [97] shows the optimum efficiency and gain of 92% and 5 dBi, respectively.

TABLE VI. COMPARISON ON THE PERFORMANCE PARAMETERS OF FREQUENCY RECONFIGURABLE BASED MIMO AND SAR ANTENNAS

Ref.	[93]	[94]	[96]	[97]
Dimensions / Material	46 × 20 × 1.6 mm^3 FR-4	120 × 60 × 1.5 mm^3 RO-4350	90 × 50 × 0.8 mm^3 FR-4	150 × 150 × 0.8 mm^3 FR-4
Isolation Level (dB)	≥ -18 dB @2.39 ~2.48 GHz and 5.15 ~6.4 GHz (Off state)	≥ -12 dB @1.77 ~2.51 GHz ≥ -25 dB @0.75 ~7.65 GHz	≥ -47 dB @2.3 ~2.4 GHz (for D1 and D2 On-state), ≥ -30.8 dB @3.4 ~3.6 GHz (for D3 On-state), ≥ -43 dB @2.5 ~2.7 GHz (for D1 and d4 On-state)	≥ -20 dB @1.6 ~1.9 GHz (Off state) ≥ -20 dB @2.2 ~2.96 GHz (On state)
Applied Approach	RF MEMS Switches	Biasing network and varactor diodes per component	DC biasing network and pin diodes and	Biasing network and pin diodes switches
Efficiency / Gain	83% / 2.9dBi	65~81 % / 0.5~3.2 dBi	48.43~73.1% / 1.99~2.78dBi	55~83 % (Lower band) 75~92 % (Upper band) / 3~5dBi
No. of Ports / Applications	Quad Ports / WLAN	Five Ports / UWB and cognitive radio (CR)	Quad Ports / WiMAX	Triple Ports / LTE and portable wireless DTV media players
Remarks	Complex layout	Expensive substrate Complex layout	Highest isolation	Optimum efficiency and gain

F. FREQUENCY-SELECTIVE SURFACE (FSS) DECOUPLING METHOD

FSS approaches can efficiently improve the isolation. However, they are discordant with low-profile structures, and they affect the radiation pattern [98]. This technique can be applied between the dielectric resonator antennas (DRA). This is obtained by accommodating an FSS between the DRAs that have been placed in the H-plane. The FSS contains an array of SRR cells that are embedded onto the E-plane. The SRR formation is modeled to achieve band-stop functionality inside the antenna frequency band.

G. ELECTROMAGNETIC BANDGAP (EBG) DECOUPLING STRUCTURE

An EBG structure blocks electromagnetic waves of a certain frequency or plays as a region to pass electromagnetic waves [99]. Various stop-band, pass-

band, and band-gap frequencies can be recognized [100]. The EBG is a periodic adjustment of dielectric or metallic materials. Structure's periodicity and singular resonance of the elements can produce many bandgaps [101]. EBG presents parasitic inductance and capacitance. Thus, the phase constant of an electromagnetic wave distributing under the patch will be much greater than the transverse electromagnetic mode. As a result, the EBG element operates in a slow-wave medium with a wavelength shorter than the transverse electromagnetic mode. Conventionally, the EBG structure is located between the antenna arrays. While, for isolation improvement, the antenna array is enclosed via the EBG.

In the literature, several types of the EBG decoupling structures have been presented and discussed recently to improve decoupling between the array antennas in MIMO and SAR systems such as the mushroom type EBG [102], dual-layer multi-element EBG [103], periodic *Z*-formed EBG [104], and 1-D and SRR EBG [105]. Table VII provides an overview of the presented EM band-gap technique-based MIMO and SAR antennas. Simplest structure with easy manufacture providing the highest isolation in order of -53.7 dB has been presented in [104]. The maximum efficiency of applying SRR and EBG has been presented in [105].

TABLE VII. COMPARISON ON THE PERFORMANCE PARAMETERS OF ELECTROMAGNETIC BANDGAP BASED MIMO AND SAR ANTENNAS

Ref.	**[102]**	**[103]**	**[104]**	**[105]**
Dimensions / Substrate	95 × 95 × 2.284 mm^3 Rogers RO4350B	35 × 40 × 1.6 mm^3 FR-4	90 × 45 × 1.6 mm^3 FR-4	60 × 57 × 1.2 mm^3 FR-4
Isolation Level (dB)	≥ -25 dB @ 2.395 ~2.42 GHz	≥ -28 dB @ 2.45 ~2.55 GHz	≥ -30.35 dB @ 5.59 GHz	≥ -53.7 dB @ 2.43 ~2.54 GHz
Applied Approach	Vias and S-EBG	Dual layer mushroom EBG	8 Z-formed EBG	SRR and EBG
Efficiency / Gain	56.57% / 5.12dBi	64.42~66.94 % 4.55~4.92 dBi	NG / 2.42dBi	82% / NG
No. of Ports / Applications	Quad Ports / IMS	Dual Ports / IMS	Dual Ports / WLAN	Dual Ports / ISM
Remarks	Complex layout	Sorely complex layout and compact dimension	Simple layout and large dimension	High efficiency and simple layout

All the approaches discussed above are summarized in Table VIII. From this table, most of them present isolation in order of 15dB, whereas the neutralization line method has the lowest isolation of 12dB. The benefits and drawbacks of several methods are listed in Table IX. The isolation value corresponds to the sort of antennas and the adopted ground plane.

TABLE VIII. COMPSRISON AMONG VARIOUS DECOUPLING MECHANISM WITH PERFORMANCE PARAMETERS

Ref.	Isolation technique	Isolation shape	Frequency	Isolation	Gain	Size
[77]	Decoupling network	Two section transmission line	746–787 MHz	23 dB	3 dBi	55×110 mm^2
[48]	Decoupling network	T-shaped strip	1.65-1.9 GHz and 2.68-6.25 GHz	10 and 15 dB	1.35 and 4.22 dBi	55×110 mm^2
[49]	Decoupling network	Tunable and coupling network	2.4 GHz	20 dB	-	90 × 72 mm^2
[52]	Decoupling network	Tunable and coupling network	2.2-2.7 and 4.9-5.9 GHz	15 dB	2.9-4.5 dBi	40 × 40 mm^2
[53]	Decoupling network	Structure with lumped element	770 MHz	16 dB	-3.8 dBi	120×50 mm^2
[55]	Parasitic elements	Structure between antenna	2.4-2.485 GHz 3.2–3.5 GHz 5.15-5.85 GHz	16 dB	-	100×60 mm^2
[103]	Parasitic elements	Branch element/resonator	3–8.5 GHz	15 dB	5.75 dBi	26×40.5 mm^2
[107]	Parasitic elements	Branch element/resonator	800–2700 MHz	36 dB	3.2 dBi	-
[108]	DGS	Slotting	2.4-2.484 GHz	17.8 dB	3 dB	39.5×20 mm^2
[109]	DGS	Defected ground plane/partial ground	2.0–7.31 GHz	17 dB	3.67 dBi	54.82 × 96.9 mm^2
[85]	Neutralization lines	Simple line	2.4 GHz	19 dB	2.1 dBi	30 × 65 mm^2
[110]	Neutralization lines	Branch line/suspended line	760 MHz	12 dB	0.9 dBi	46 × 85 mm^2

TABLE IX. BENEFITS AND DRAWBACKS OF ISOLATION TECHNIQUES

Ref.	Techniques	Benefit	Drawback
[39] – [59]	Decoupling network	- Easy decoupling structure - Enhance far-field properties	- Sometimes additional space is needed - Generate ohmic losses
[60] – [70]	Parasitic elements	- Control the isolation - Suitable DG	- Shift in frequency due to parasitic elements
[71] – [82]	Defected ground structure (DGS)	- Small antenna dimension - Proper diversity	- usually not suited for mobile applications - Low gain
[84] – [89]	Neutralization lines	- Acceptable impedance matching - Proper diversity with DG	- Lower frequency band - Shorter bandwidth when compared with upper frequency band
[90] – [97]	PIN diode, Varactor diode and feeding arrangement	- Appropriate isolation - High gain	- Losses due to component - Short frequency band - Complex configuration
[99] – [105]	Electromagnetic Bandgap (EBG)	- Easy layout - Acceptable isolation	- Short bandwidth - Low gain

IV. HIGH EFFICIENT DECOUPLING TECHNIQUES BASED ON THE METASURFACE (MTS) AND METAMATERIAL (MTM) PROPERTIES APPLICABLE IN SAR AND MIMO ANTENNA SYSTEMS WITH WIDE RANGE OF DESIGN POSSIBILITIES

The results presented in Section II and listed in Tables I - IX show that the abovementioned decoupling approaches are just presented for a limited number of the array elements. In addition, the design process of some of them is complex and far way to practical realizations. Most of them are working at a specific range of frequency with low gain and efficiency, and they have affected the total physical size of the array antennas. In addition, they are not applicable for a wide range of design possibilities, and they have an asymmetric configuration which enables them for mass production.

Waveguide slot array (WSA) antennas propose favorable properties that contain moderate cost, low-loss, and high power-handling ability [111]. While the major disadvantage of the WSA is the interferences between the slit antennas that reduce the bandwidth, gain, and recurves the radiation pattern. To employ WSA antennas in next generation SAR and MIMO systems, a low degree of coupling is required [112]. Several methods have been implemented to increase isolation [113-128]. Some commonly used methods include coplanar strip walls between the antennas [129-130] and frequency selective surfaces [131]. However, these methods diminish the radiation pattern. This happens because a coplanar strip wall or an FSS wall does not have a good matching condition. Consequently, the radiation pattern is degraded because of reflected waves from the integrated wall between the antennas.

Therefore, in this part of the review study the new approaches are introduced to increment isolation between WSA antennas. These primarily involve placing an MTS between the waveguide slit antennas. Proposed techniques are exhibited to significantly repress the mutual coupling and increase the gain and working frequency band. They are effective and simple to implement.

Besides the metasurface- and metamaterial-inspired decoupling methods applied to WSA antennas, other efficient decoupling approaches based on the same concepts have been presented in bellow with providing an efficient number of examples and various type of designs for SAR and MIMO applications. The main advantages of the following designs are their simple prototypes with ease of manufacture process, low cost, high isolation level between the array elements, as well as, not being limited to small number of array elements, being applicable for a wide range of frequency band, having very negligible effects on the performance parameters with keeping constant the physical dimensions, and having symmetrical layouts which enable them for cost effective mass production.

A. MUTUAL-COUPLING REDUCTION BETWEEN WSA ANTENNAS INSPIRED MTS BULKHEAD FOR MIMO SYSTEMS

In [113], a novel mechanism has been presented to suppress the interferences between WSA antennas based on the MTS concept. This is obtained by locating an MTS bulkhead between the antennas, as depicted in Fig.2. The antenna's performance is displayed to improve when compared to the same reference structure with no MTS. The implemented antennas have a physical dimension of 40 mm × 20 mm × 5 mm and operate over a bandwidth of 1.7 GHz to 3.66 GHz, which relates to a practical bandwidth of 73.13%. The reference WSA antennas present an average isolation of -20 dB, while, with an MTS bulkhead, the decoupling is depicted to enhance to -36.5 dB. Furthermore, the bandwidth expands by ~10%, and the gain increases by 14.66%. This mechanism will be very suitable for SAR and MIMO antenna systems where low coupling between adjacent radiation elements is necessary to improve the specifications of the structure and minimize array phase errors, as a necessity to increment the performance of the system.

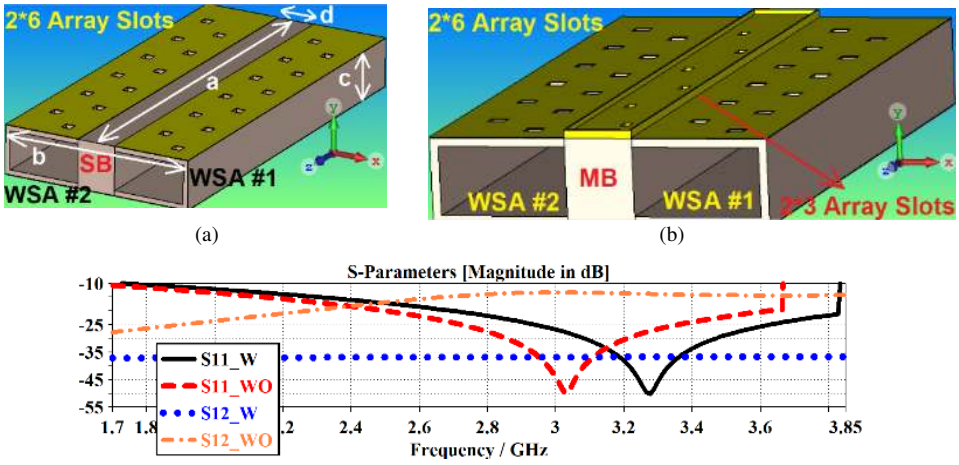

Fig.2. (a) Reference structure, (b) WSA antennas with MTS bulkhead, (c) reflection and transmission coefficients. WO and W represent without and with MTS bulkhead, respectively [113].

B. REDUCTION IN INTERACTION BETWEEN LONGITUDINAL-SLOTTED ARRAY BASED ON SIW ANTENNA LOADED WITH METAL-FENCES OPERATING ACROSS VHF/UHF FREQUENCY-BANDS

In [114], it is investigated that substrate integrated waveguide longitudinal slotted array antenna (SIWLSAA) that is loaded with metal fences shows low mutual coupling throughout VHF/UHF bands. A reference SIWLSAA implemented for comparison aim includes 3×6 slotted arrays designed on the top-side, and the bottom-side of the FR-4 layer has the lowest mutual coupling of -63 dB between its slits. Suppression in mutual coupling is discussed by applying an easy, innovative way based on locating a metal fence between each row of the slit arrays. The mutual coupling is exhibited to better than -83 dB entire 0.2-1.0 GHz with a gain more than 1.5dBi, and a side-lobe level less than -40 dB. The presented SIWLSAA shown in Fig.3 is compact and has a physical dimension of 40 mm × 10 mm × 5 mm ($0.026\lambda_0 \times 0.006\lambda_0 \times 0.002\lambda_0$, where λ_0 is defined at 200 MHz). The proposed SIWLSAA will be very suitable for MIMO and radar system applications.

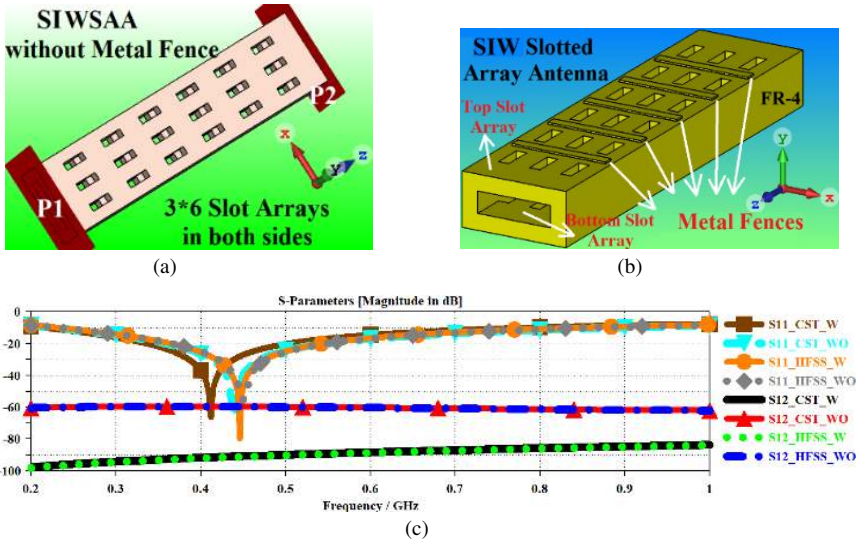

Fig.3. (a) Reference structure (WO), (b) proposed structure with metal fences (W), and (c) S-parameter performances [114].

C. ANTENNA ISOLATION ENHANCEMENT APPLYING INTEGRATED MTS ISOLATOR FOR SAR AND MIMO APPLICATIONS

In [115], a decoupling structure based on MTS that is constructed of a square-wave slot pattern with overstated corners realized on a rectangular microstrip presents low mutual coupling between neighbor antennas for array systems. The 1×2 symmetric antenna array embedded with the proposed decoupling structure, which is exhibited in Fig.4, is modeled to work at ISM bands of X, Ku, K, and Ka. As demonstrated in Fig.4, the surface current distributions indicate that the isolation structure compounded of the square-wave slit soaks up the surface waves that would otherwise couple with the adjoining radiating parts. With this mutual coupling suppression technique, the following are observed: (i) the average

isolations in the respective ISM bands mentioned above are 7, 10, 5, and 10 dB; and (ii) the center-to-center distance between the neighbor parts is decreased to 10mm (0.28λ). The average gain increment with the MTS decoupling is 2 dBi.

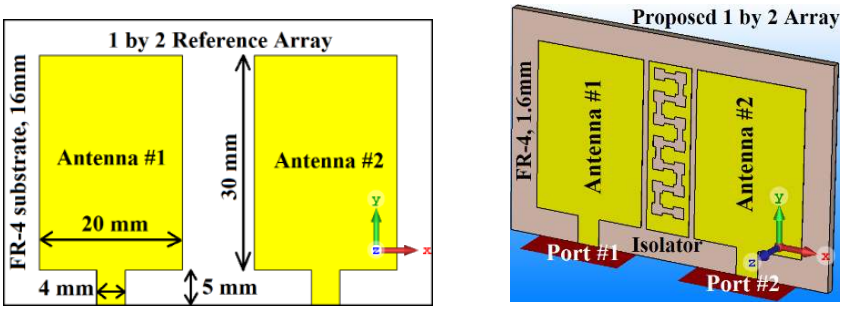

(a) (b)

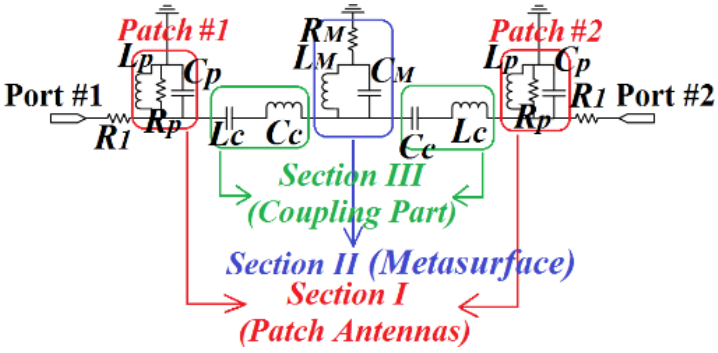

(c)

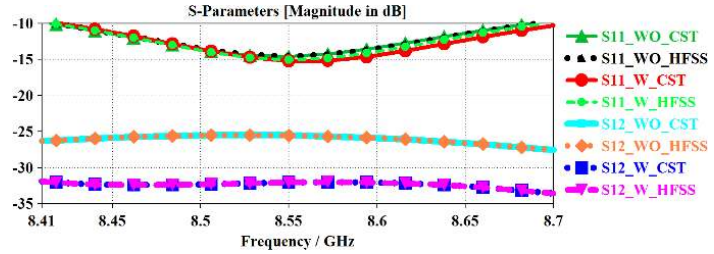

First Band

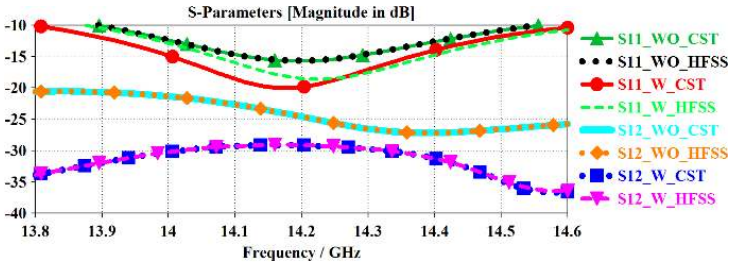

Second Band

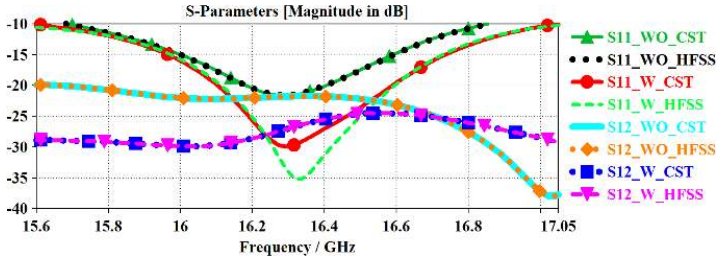

Third Band

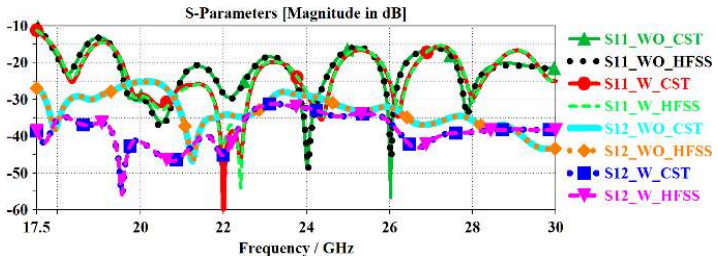

Fourth Band

(d)

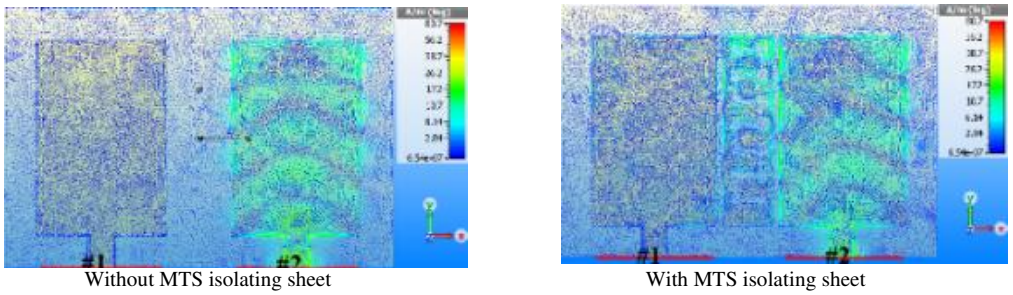

Without MTS isolating sheet

With MTS isolating sheet

(e)

Fig.4. Configuration of (a) reference array antennas (WO), (b) proposed structure applying the MTS isolating sheet (W), (c) circuit diagram, (d) S-parameters, and (e) surface current distributions at 19.5 GHz (when one port is stimulated, the other one is matched to a 50-ohm load) [115].

D. WIDEBAND HIGH ISOLATED WSA ANTENNA WORKING OVER Ku- AND K- BANDS FOR RADAR AND MIMO SYSTEMS

An innovative approach to increase the isolation between the radiating parts of a waveguide slot array antenna has been proposed and elaborated in [116]. It has obtained by realizing slits between the waveguide oval-formed slits, as shown in Fig.5. The reference array has been implemented with an organization of 3×5 oval-formed slots. With embedding linear slits between the radiating oval-formed slots in both vertical and horizontal directions, major increment in isolation has obtained to have values of 24, 20, and 32 dB over the bands of 12.95 to 13.75 GHz (Ku-band), 15.45 to 16.85 GHz (Ku-band), and 18.85 to 23.0 GHz (K-band), respectively. The study on the surface current distributions displays that the slits act as an isolating architecture that soaks up the surface waves, which would be coupled with the adjacent elements. The center-to-center gap between the slits is 0.2λ that is at least two times less than the traditional array structures. Using the slit decouplings, the lowest and highest gains increase by 53.5% and 25.5%. Furthermore, the radiation patterns are unchanged. This technique is easy for employment and inexpensive for mass production.

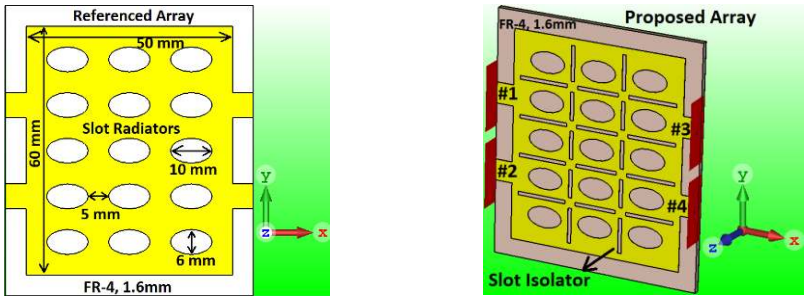

(a) (b)

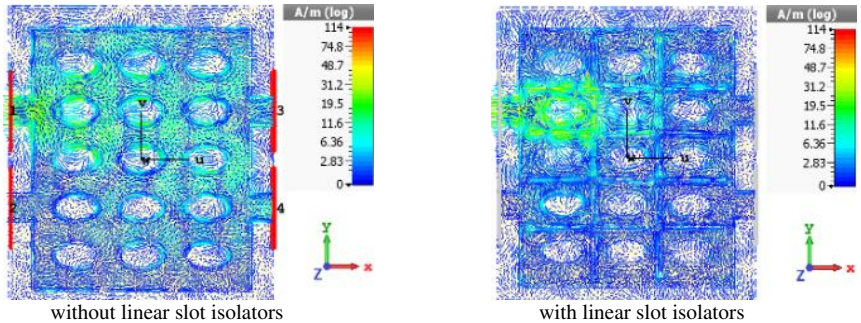

without linear slot isolators

with linear slot isolators

(c)

This article has been accepted for publication in a future issue of this journal, but has not been fully edited. Content may change prior to final publication. Citation information: DOI 10.1109/ACCESS.2020.3032826, IEEE Access

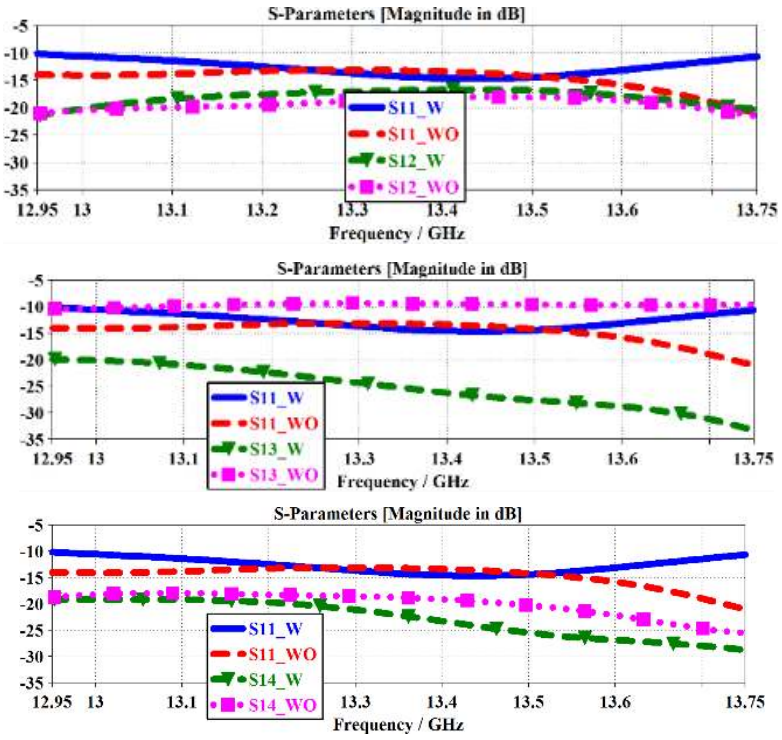

First band, 12.95 - 13.75 GHz (Ku-band)

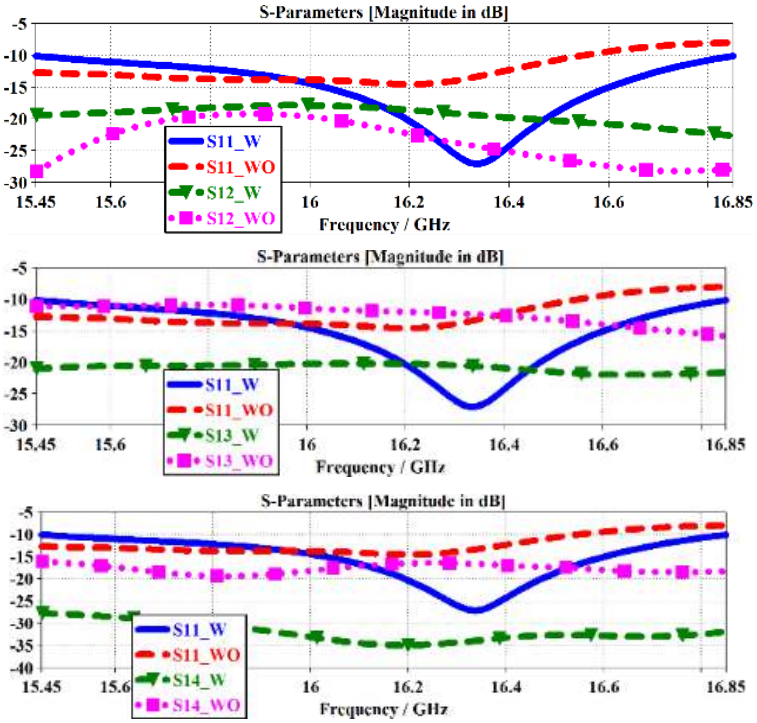

Second band, 15.45 - 16.85 GHz (Ku-band)

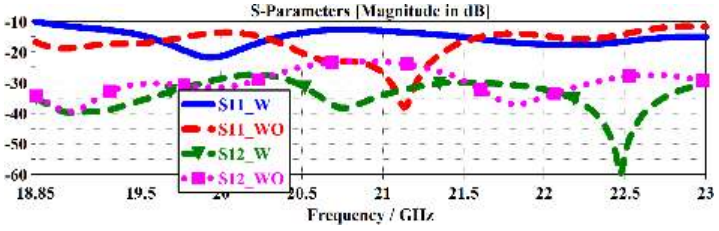

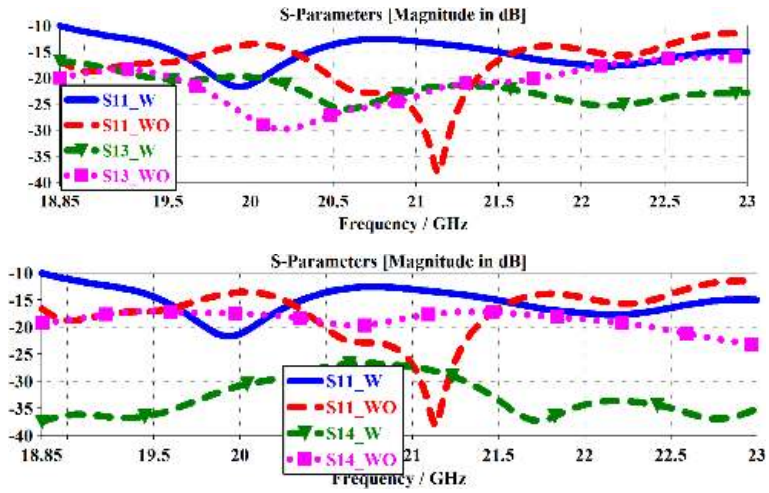

Third band, 18.85 - 23 GHz (K-band)

(d)

Fig.5. (a) Reference structure (WO), (b) proposed structure with (W) linear slot isolators, (c) surface current distributions at 22.5 GHz (when one port is stimulated, the others are matched to a 50-ohm load), and (d) S-parameters [116].

E. EM DECOUPLING INSPIRED MTM CONTENT IN ANTENNA ARRAY SYSTEM TO SUPPORT FULL-DUPLEX APPLICATION

An electromagnetic technique to suppress the coupling between array antennas applying MTM EBG is presented and discussed in [117]. Fig.6 shows that the proposed configuration can be considered for a full-duplex array antenna system with short distances between the array elements ($0.33\lambda_0$) without any decay in the radiation pattern. By implementing this way, the decoupling is exhibited to increment by >30 dB in the array structure containing three patches modeled to work over 9.7 - 12.3 GHz. To more in-depth discernment, the E-field magnitude profiles without and with the MTM-EBG isolating structure are displayed in Fig.6. Obviously, the distributing E-field is not permitted to be coupled to the neighbor elements that affirms the efficiency of the presented method in decreasing surface waves. A parametric evaluation was utilized to maximize the isolation performances. The array structure has the physical and electrical sizes of 65 mm × 22.5 mm ×1.6 mm and $2.16\lambda_0 \times 0.75\lambda_0 \times 0.053\lambda_0$, respectively, where λ_0 is defined at the mid-band of 10 GHz.

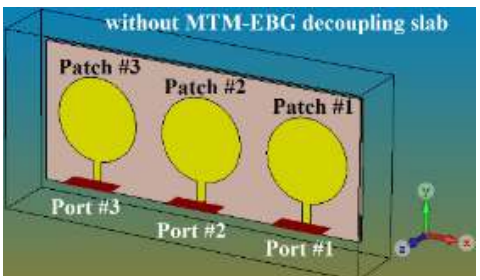

(a)

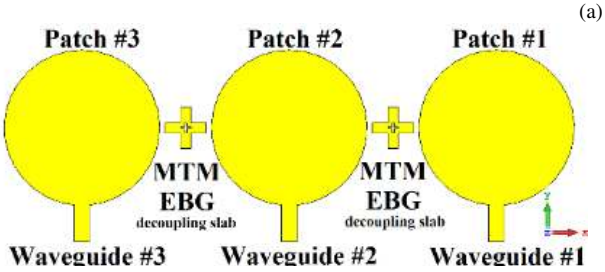

(b)

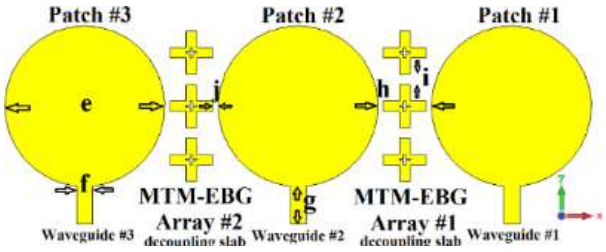

(c)

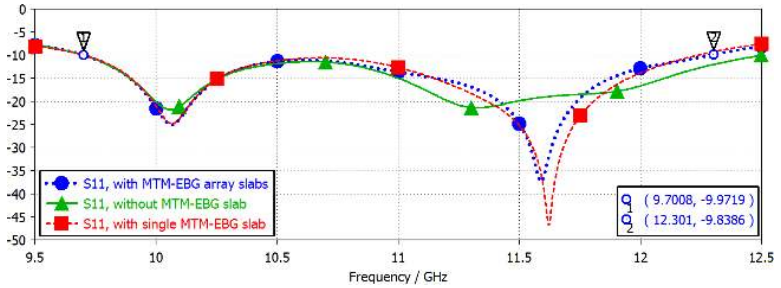

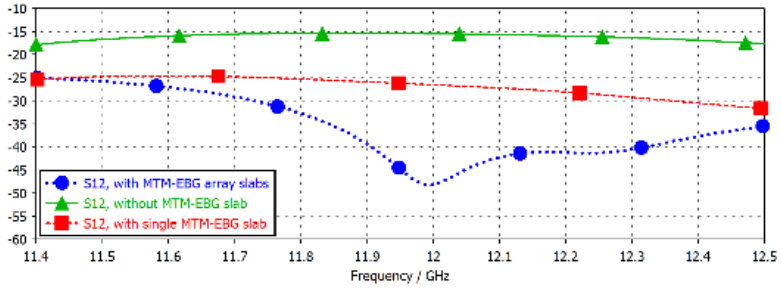

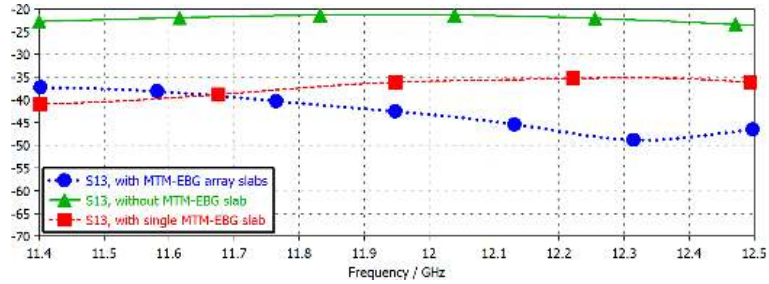

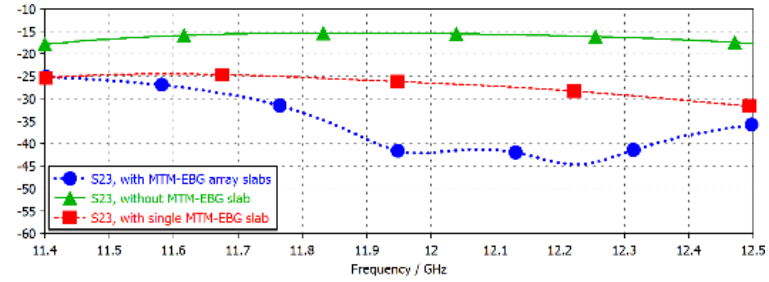

(d)

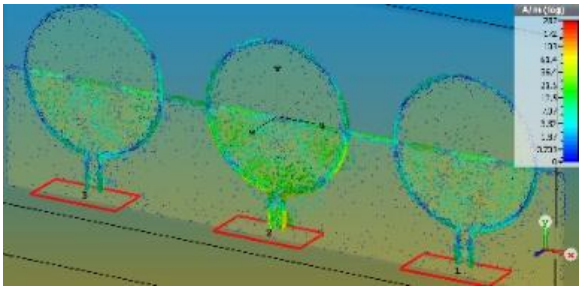

without MTM-EBG decoupling slab

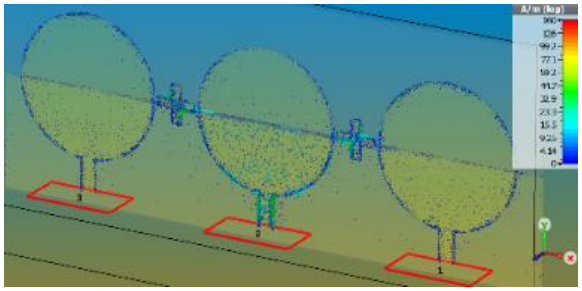

with single MTM-EBG decoupling slabs

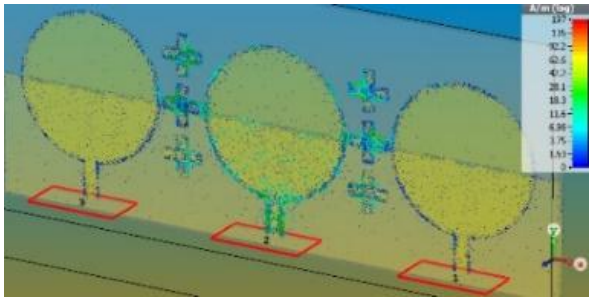

with array of MTM-EBG decoupling slabs

(e)

Fig.6. (a) Reference antenna array, (b) antenna array with single MTM-EBG decoupling slabs, (c) proposed antenna array with array of MTM-EBG decoupling slabs, (d) S-parameters performances, (e) distributed surface currents at resonance frequency of 10 GHz [117].

F. ISOLATION ENHANCEMENT IN MTM SIW SLOTTED ANTENNA ARRAYS EMPLOYING METAL-FENCE DECOUPLING SLABS FOR SAR AND MIMO APPLICATIONS

A novel sort of decoupling approach is realized to an MTM substrate integrated waveguide (SIW) slotted antenna array in [118]. Fig.7 shows that the circular formed reference SIW antenna array is built from an Alumina layer with a physical size of 40 mm × 5 mm × 1.5 mm. Integrated into the reference structure are 38 slits with the same size, i.e., 2 mm × 1 mm × 1.5 mm. This structure workes across X-band to Ku-band, providing an average mutual coupling of about -10dB. The mutual coupling was suppressed through embedding metal fence decouplings between the radiation slits, which degraded the interferences by an average of 13dB. Furthermore, the impedance matching bandwidth is improved without decay in the radiation patterns. By utilizing the metal fence decouplings, the optimum obtained gain enhances by ~10%. The proposed approach is easy to realize, and it has been presented for SAR and MIMO systems.

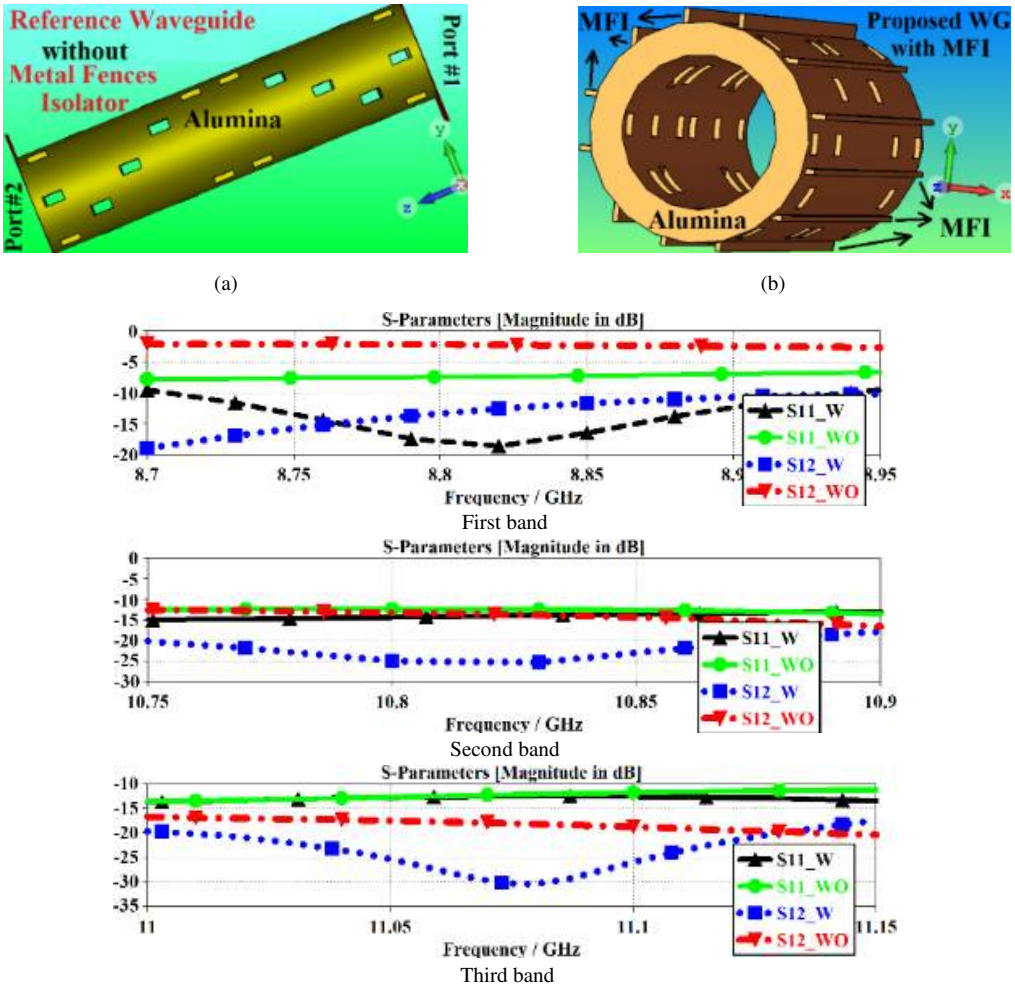

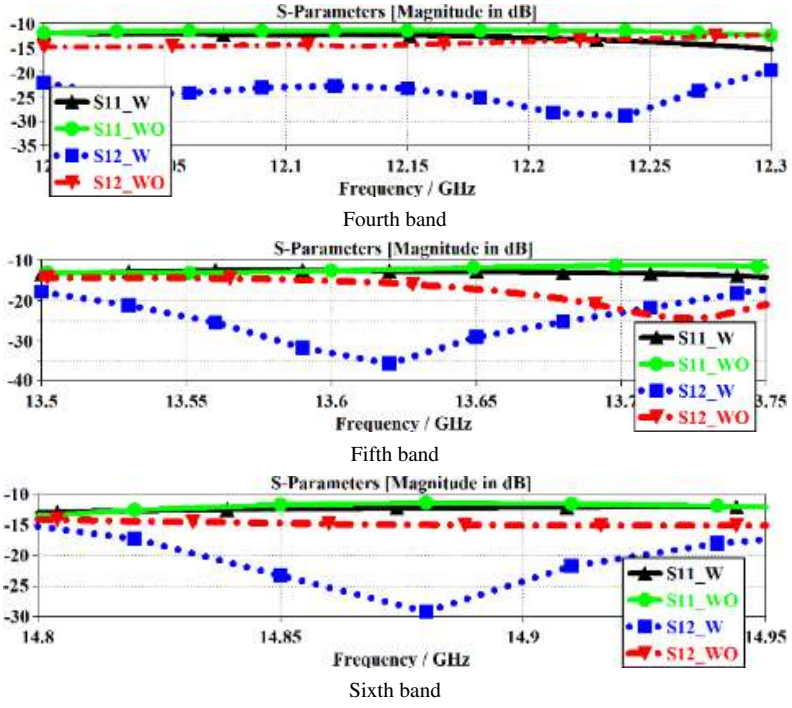

(c)

Fig.7. Geometries of (a) the reference structure (WO) and (b) the proposed structure with MFIs (W), and (c) S-parameter responses [118].

G. SUPPRESSION IN MUTUAL COUPLING APPLYING MTM SUPERSUBSTRATE FOR HIGH PERFORMANCE & DENSELY PACKED PLANAR PHASED ARRAYS

In [119], an efficient decoupling method is illustrated for a phased array. It is obtained via placing a MTM superstrate patch between the radiation parts of the phased array, as shown in Fig.8. The patch is implemented through integrating slits within the patch, where the slits are organized in a 2×3 array. This technique is applied to an FR-4 layer. An average isolation improvement of 5dB is obtained throughout its working bandwidth. This approach is: (i) easy to realize; (ii) suitable for planar antenna designs; (iii) simply applicable in practice; (iv) resilient and dominates the deficiencies of poor front-to-back ratio already presented in literature; and (v) appropriate for densely packed microstrip. Additionally, the presented method is exceptionally versatile for many applications having precise performance necessities.

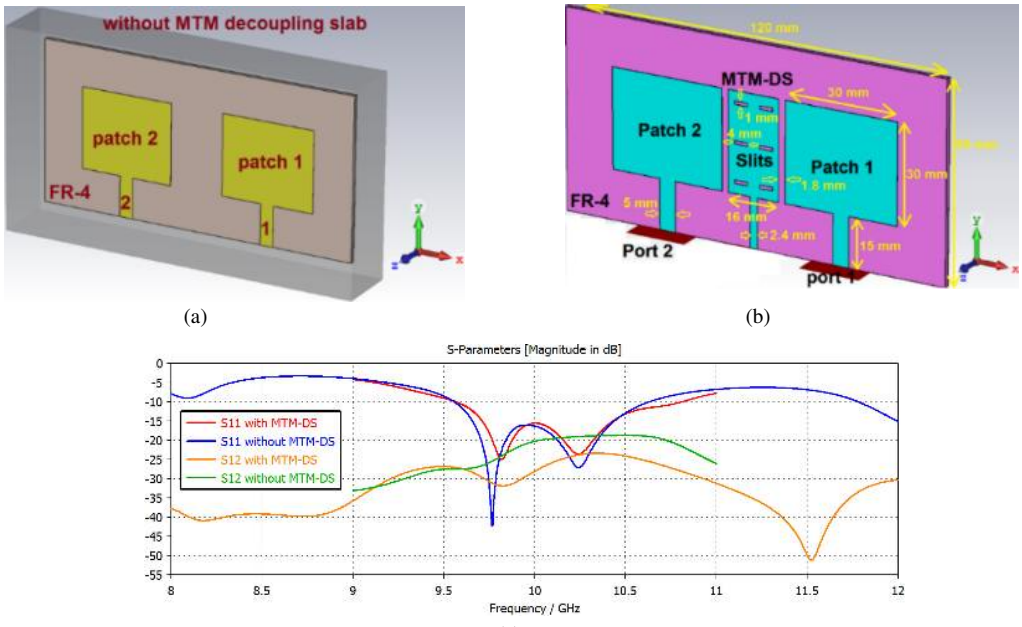

(a) (b)

(c)

Fig.8. Layout of the antenna (a) without and (b) with MTM decoupling super substrate, and (c) S-parameters [119].

H. HIGH ISOLATED ARRAY ANTENNAS FOR SAR APPLICATIONS OVER X- AND Ku- BANDS

Modern MIMO and SAR need a frequency band which is larger than 1 GHz. Waveguide slot antennas are popularly utilized in MIMO and SAR systems because of their intrinsic benefits, namely power handling ability and high efficiency. However, these antennas have a confined frequency band. While the frequency band of slot antennas can be expanded through applying ridge waveguides, this way presents fabricating intricacy and is not cost-effective. An innovative solution has been proposed in [120] to implement a wide frequency band via applying a 2×3 array structure with the isolation between the antenna incremented by embedding a decoupling wall between the radiating antennas, as shown in Fig.9. The decoupling wall contains three intercoupled U-shaped microstrip transmission lines. By this method, the frequency band is wider than 2 GHz within the X-band and Ku-band.

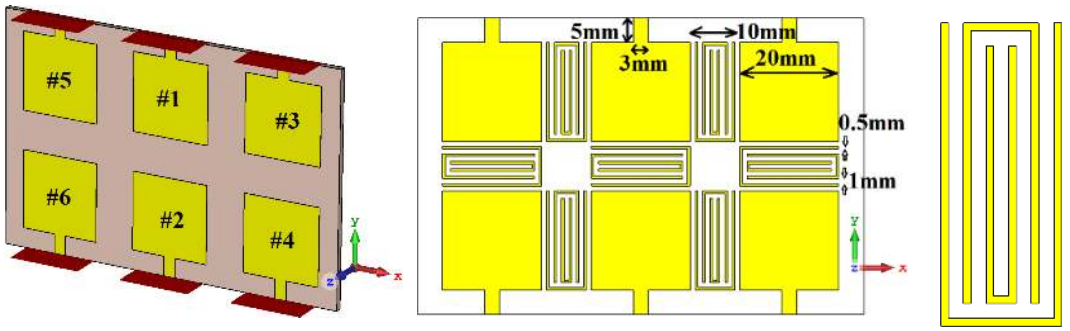

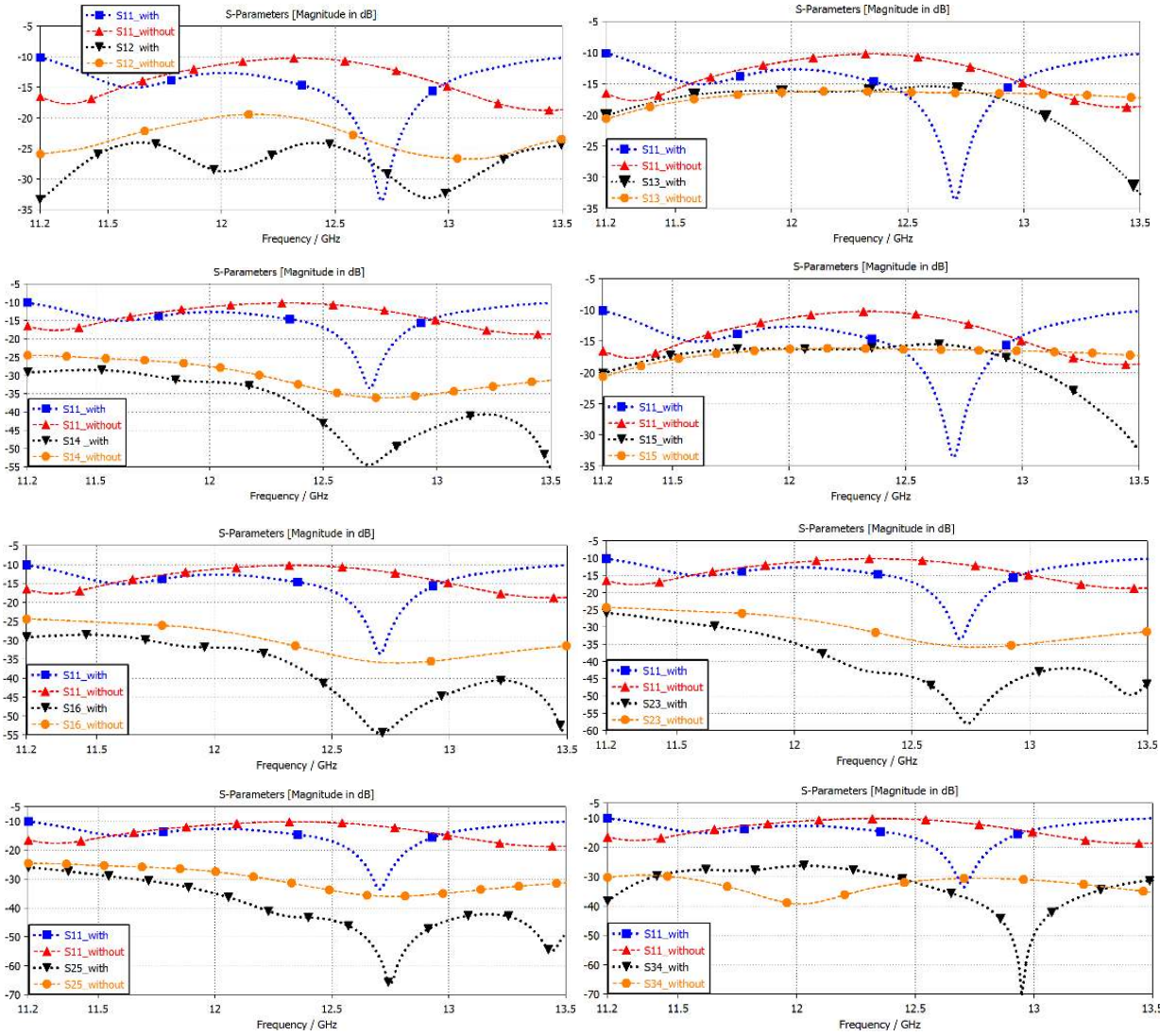

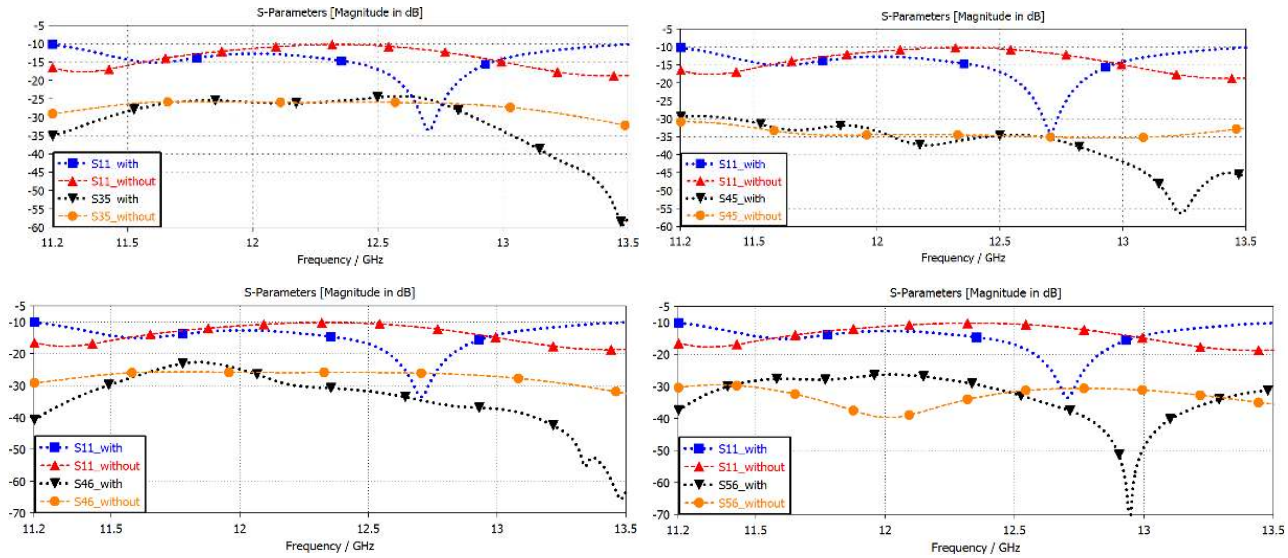

(d)

Fig.9. (a) Reference array antennas without isolation wall, (b) proposed array antennas with isolator wall, (c) isolator wall, (d) S-parameters [120].

I. DECOUPLING APPROACH INSPIRED MTM SUPERSUBSTRATE UTILIZED IN DENSELY PACKED ANTENNA ARRAYS

An easy and feasible mechanism for increasing the isolation between neighbor antennas is proposed and applied in [121]. Fig.10 shows that this is achieved by placing a smaller patch with MTM isolating structure between the antennas. The antenna structures are circular patches and the MTM decoupling structure is designed from a hexagonal slot resonator. The direct effect of realizing the MTM decoupling structure is 60% improvement in isolation between the closely spaced elements, 200% enhancement in impedance match, and 369% enhancement in the practical bandwidth. Because GND is unchanged, the front-to-back ratio is unaltered as well. The method is simply feasible and is efficiently applicable in beam scanning systems.

(a)

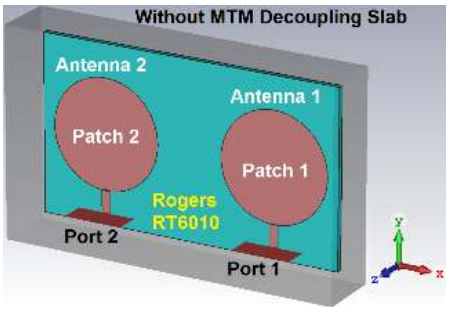

(b)

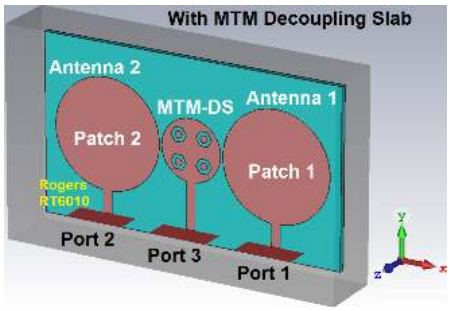

(c)

This article has been accepted for publication in a future issue of this journal, but has not been fully edited. Content may change prior to final publication. Citation information: DOI 10.1109/ACCESS.2020.3032826, IEEE Access

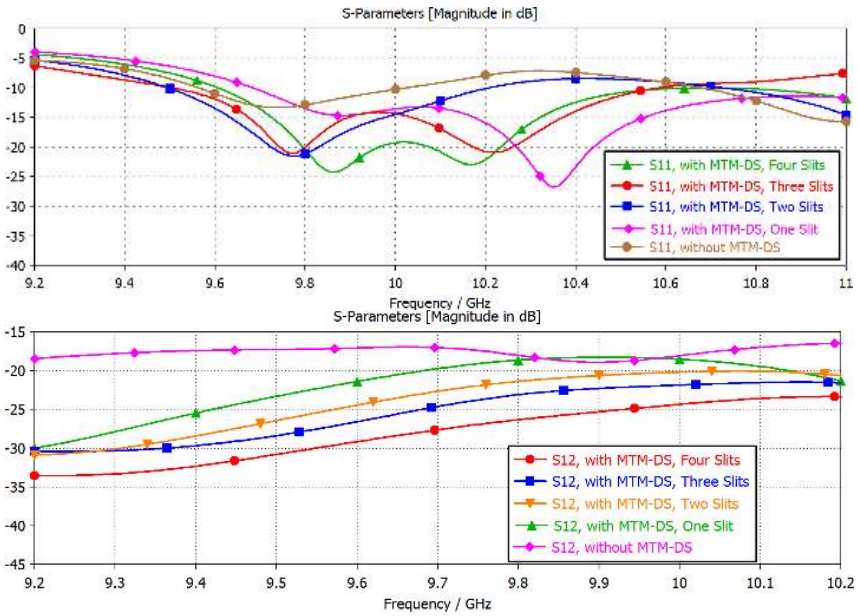

(d)

Fig.10. (a) MTM isolation sheets, (b) structure without MTM isolation sheet, (c) with multiple MTM isolation sheet, and (d) S-parameters [121].

V. COMBINED ISOLATION TECHNIQUES

In this section, to achieve high and stable isolation between the radiation elements throughout the operating frequency band without affecting other performance parameters such as array's dimensions, bandwidth, and radiation properties, new array antennas based on combined isolation techniques are proposed, designed and manufactured. In other words, the proposed decoupling slabs located between the radiation elements for these new array antennas are realized based on the combination of the metasurface and metamaterial and electromagnetic bandgap concepts. As a result, high and stable isolations over entire bandwidths are achieved. The proposed works are discussed as follows.

A. INTERFERENCE REDUCTION BETWEEN CLOSELY PLACED ANTENNAS APPLYING EBG MTM FRACTAL LOADING

In [122], an efficient method is investigated to increase the isolation between the closely spaced antennas. It has been obtained by incorporating a fractal decoupling slab between the radiating patches, as displayed in Fig.11. The fractal isolating sheet is an EBG frame based on MTM. By adopting this way, the space between the patches has decreased to 0.65λ for isolation improvement at amounts up to 37, 21, 20, and 31dB at the X-, Ku-, K-, and Ka-bands, respectively, without decay in the radiation patterns. Two-element antennas are exhibited to work across a large frequency band, i.e., 8.7 to 11.7 GHz, 11.9 to 14.6 GHz, 15.6 to 17.1 GHz, 22 to 26 GHz, and 29 to 34.2 GHz. An optimum gain increment in order of 71% has been achieved. The current density distributions demonstrate that the surface currents are decreased by presenting the fractal load between the adjacent elements. This affirms the realized decoupling structure behaves as an efficient isolation frame. The specifications of the antenna have been validated by experimental results. This approach can be used in several of the previously mentioned applications, and it is also suitable for adjacent antennas in arrays found in Radar, MIMO, and RFID systems.

(a)

(b)

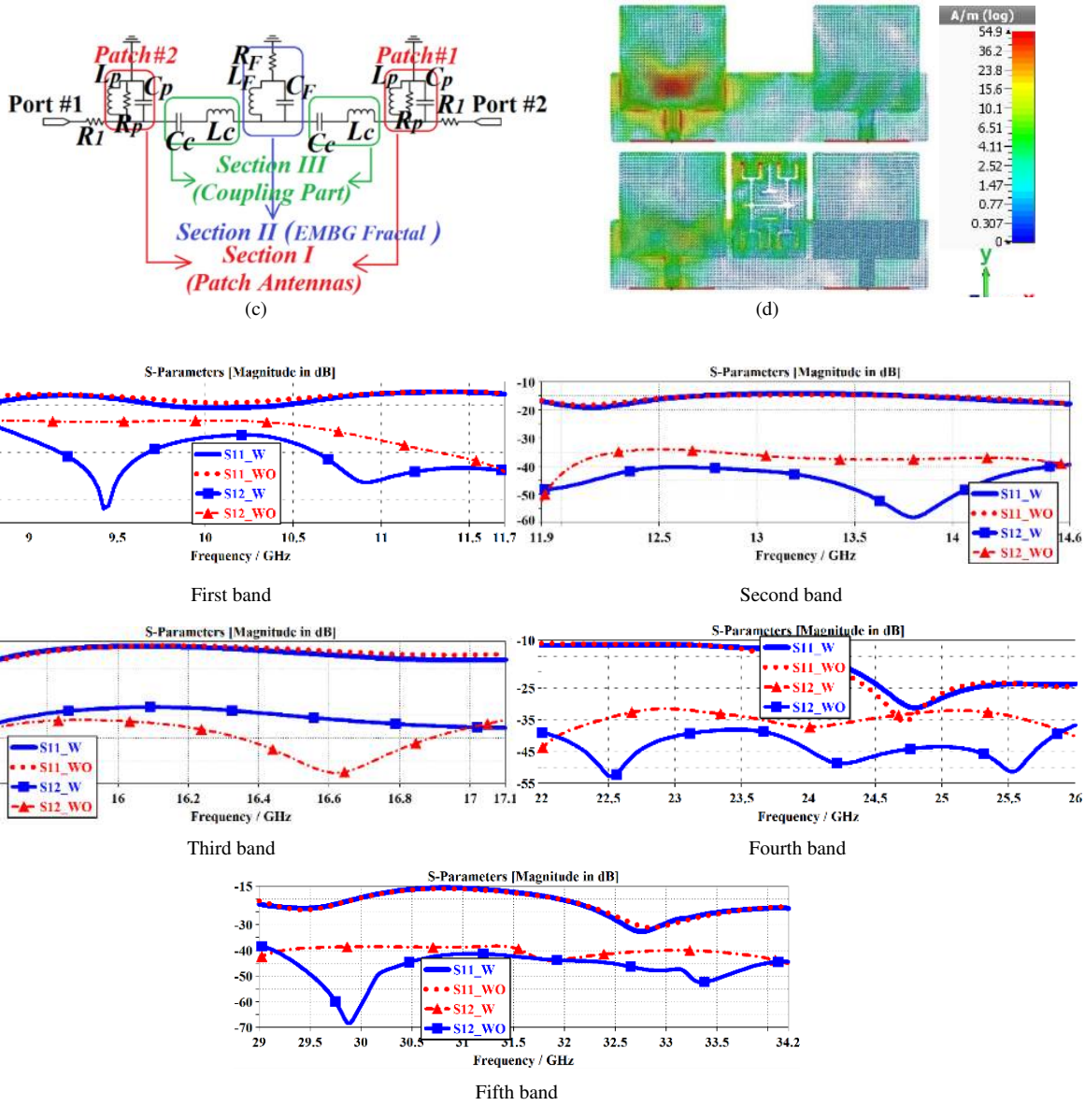

Fig.11. (a) reference array (WO), (b) proposed array with EBG fractal decoupling sheet (W), (c) equivalent circuit diagram, (d) surface current distribution at 29.9 GHz, and (e) measured S-parameters [122].

B. STUDY ON MUTUAL COUPLING REDUCTION BETWEEN ADJACENT ARRAY ANTENNAS WITH REALIZATION OF FRACTAL MTM EBG ARCHITECTURE

The abovementioned technique presented in [122] was further developed and extended to a 2×2 antenna array with radiation elements in [123]. In [123], a decoupling MTM geometry based on fractal EBG frame, as displayed in Fig.12, considerably suppresses the coupling between the antennas. The assemblage of the MTM-EBG layout is cross-formed with fractal-formed slits engraved in each arm of the cross. The fractals are compounded of four interjoined 'Y-formed slits, which have separated with an inverted 'T-formed slit. The MTM-EMBG frame is located between the singular elements in a 2×2 array antennas. The experimental data illustrate the average isolation improvement across the operating bandwidth is 17, 37, and 17 dB between the antennas 1 and 2, 1 and 3, and 1 and 4, respectively. For this mechanism, metallic-via-holes are not required. The antenna array supports the bandwidth of 8 - 9.25 GHz for X-band operations, which relates to a practical bandwidth of 14.5%. The center-to-center distance between the neighbour antennas has decreased to $0.5\lambda_0$ without decay in the radiation patterns. The empirical gain changes between 4 and 7 dBi, and the radiation efficiency alters from 74.22% to 88.71%. This technique is feasible in the realization of neighbour antenna arrays applied in MIMO and SAR devices.

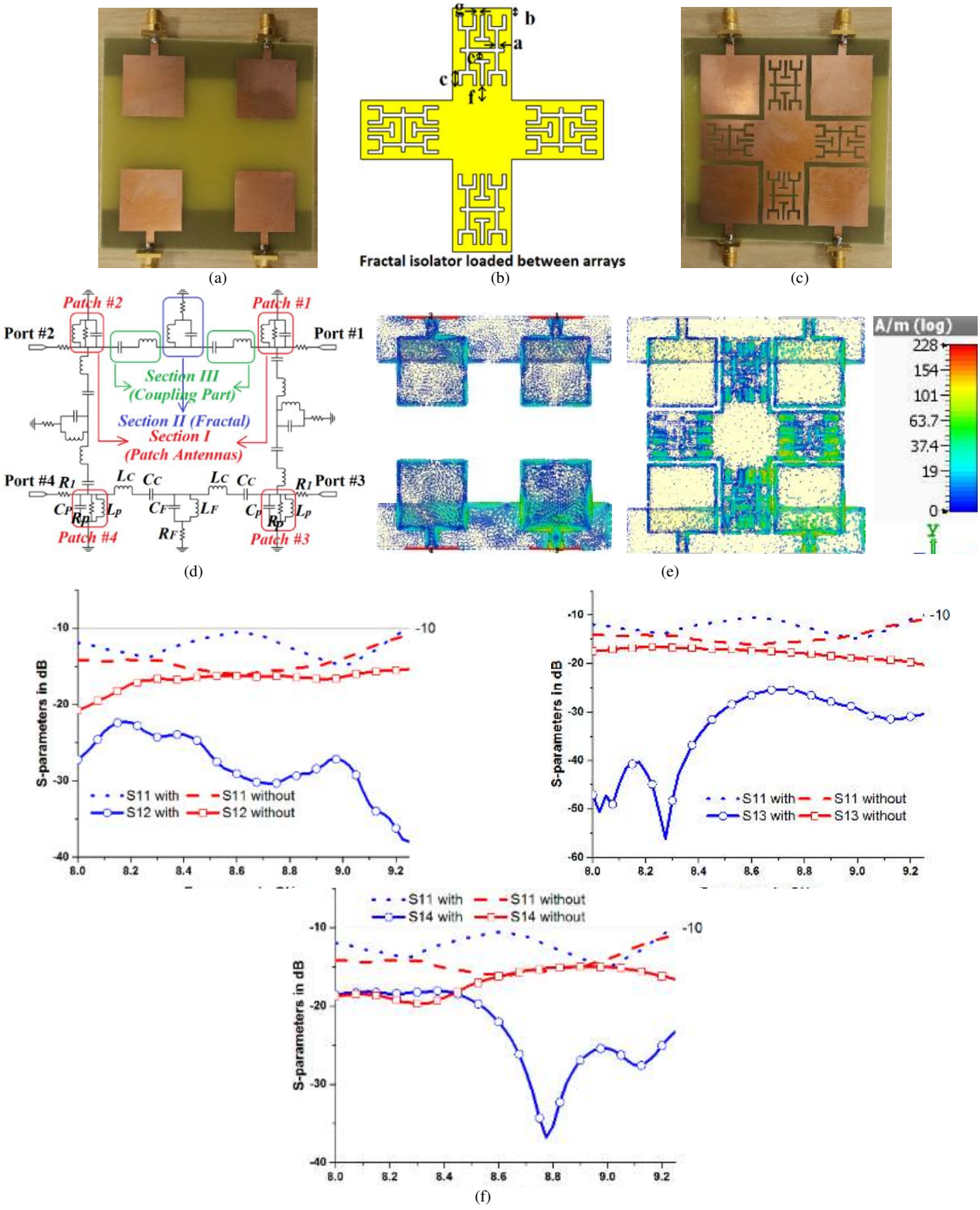

Fig.12. (a) reference 2×2 antenna array, (b) crossed-shaped fractal decoupling structure, (c) proposed 2×2 array antennas with fractal isolator loading, (d) equivalent circuit diagram, (e) surface current density distributions without and with fractal isolator loading at 8.85 GHz, and (f) empirical S-parameters, [123].

C. INTERACTION BETWEEN CLOSELY PACKED ARRAY ANTENNAS APPLYING MTS FOR MIMO AND SAR SYSTEMS

An efficient method to repress the interference between adjacent patches that is usual in densely packed antenna arrays has been proposed and demonstrated in [124]. These antennas provide frequency beam-steering ability required in MIMO and SAR systems. Fig.13 shows that the proposed technique applies an MTM decoupling slab that is incorporated between the radiating patches to increase the decoupling between the antennas that would otherwise reduce the performance parameters. The MTM decoupling slab composed of mirror imaged E-formed

slots etched on a patch with an inductive stub. Experimental data affirms that the average mutual coupling (S_{12}) is -27dB over 9 - 11 GHz without MTM decoupling slab. However, with the adoption of the MTM decoupling slab, the average mutual coupling decreases to -38dB. The distance between the antenna has decreased to $0.66\lambda_0$, where λ_0 is defined at 10GHz. Additionally, the employment of this method provides a 15% extension in the working frequency band. Furthermore, the decoupling influences are remarked through imagining the surface current distributions curves entire the antenna array. With the adoption of the MTM decoupling slab, powerful currents are induced on the patches that obviously investigates the effects of the MTM decoupling slab in reducing surface current wave interaction between the elements. At 9.95 and 10.63 GHz the gain value is 4.52 dBi and 5.40 dBi, respectively. Additionally, this way omits poor front-to-back ratio occurred in other isolating approaches, and it is comparatively easy to realize. Supposing sufficient distance is existing between the neighbor elements, the MTM decoupling slab can be embedded with available antenna arrays, which makes this technique versatile.

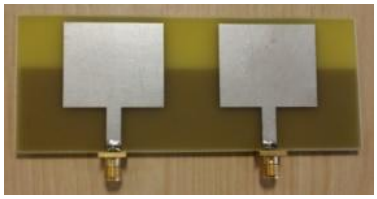

(a)

(b)

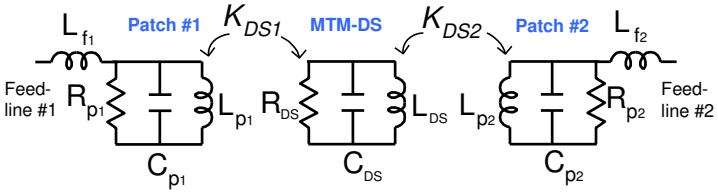

(c)

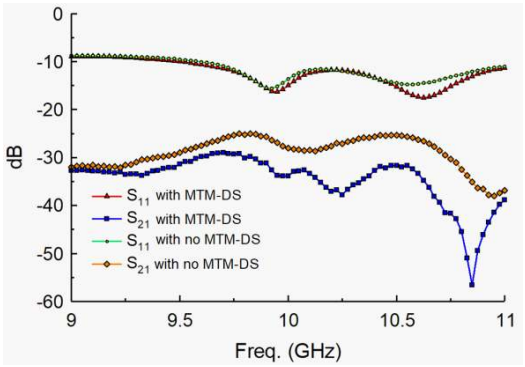

(d)

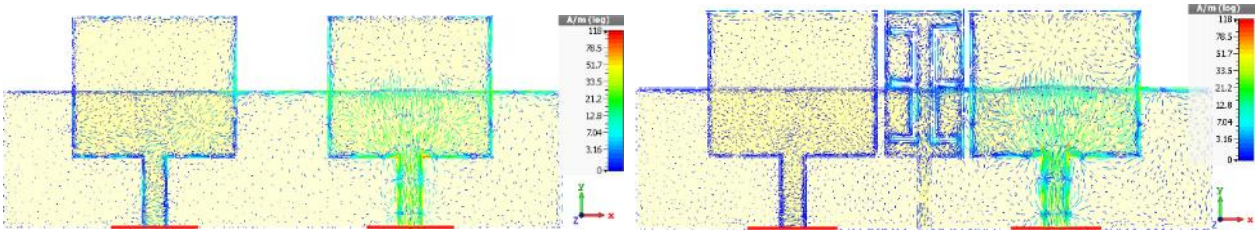

without MTM isolator shield

with MTM isolator shield

(e)

Fig.13. Antenna array (a) before apply MTM isolator shield and (b) after apply MTM isolator shield, (c) circuit of two patches with MTM-DS, (d) S-parameter responses, (e) surface current densities before and after apply MTM isolator shield at 10.65 GHz [124].

D. ISOLATION IMPROVEMENT UTILIZING INTEGRATED MTM EBG DECOUPLING SLAB FOR DENSELY PACKED ARRAY ANTENNAS

In [125], the work presented in [124] is further developed and extended from 1×2 linear array antennas, which consist of two radiation elements, to 2×2 matrix array antenna configurations, which consist of four radiation antennas. An innovative method to suppress the mutual coupling in adjacent antennas array by incorporating an MTM EBG frame in the distance between the patches to reduce surface currents that would otherwise participate in interferences between the array antennas is developed and investigated. This MTM EBG decoupling frame is a cross-formed microstrip transmission line on which two outward facing E-formed slots are imprinted as shown in Fig.14. Inverse other MTM prototypes, it is via free. The highest experimental decoupling obtained between the four-element array antennas is 60dB at 9.18 GHz. Throughout the empirical working band of 9.12 - 9.96 GHz, the lowest experimental coupling between each element is -34.2dB at 9.48 GHz, and without any decay in radiation patterns. The average experimental mutual coupling across the bandwidth is -47dB. Current density distributions explain that the MTM EBG decoupling frame soaks up the fringing fields that would otherwise couple with the neighbor radiating patches. The results shown in Fig.14 affirm this method is proper for applications in MIMO and SAR systems.

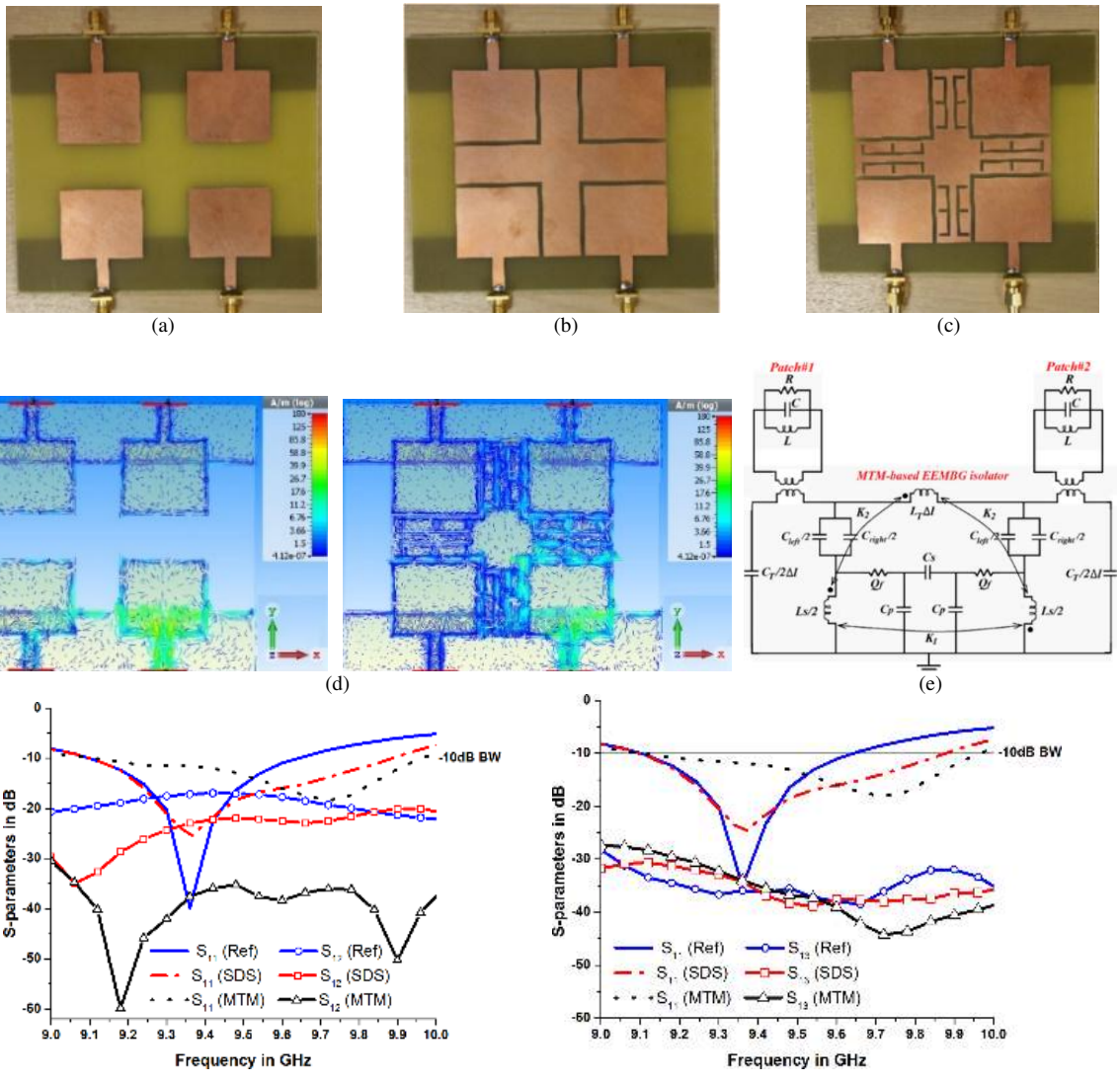

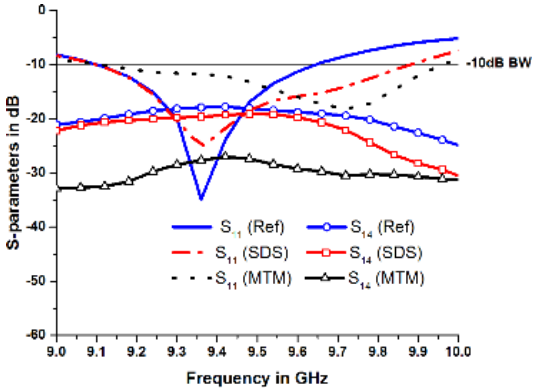

(f)

Fig.14. (a) Reference array antenna, (b) array structure with embedded simple isolator sheet, (c) array structure with embedded MTM based EBG isolator sheet, (d) current densities without and with the embedded MTM based EBG isolator sheet at 9.6 GHz, (e) circuit model, and (f) measured S-parameter responses[125].

E. CRLH MTM-BASED LEAKY-WAVE ARRAY ANTENNA WITH LOW MUTUAL COUPLING REALIZED ON SIW WITH ±30° FREQUENCY BEAM-SCATTERING ABILITY

A practical investigation to implement a novel MTM leaky-wave antenna (LWA) applied in the making of a 1×2 array that is built utilizing SIW methodology for millimeter-wave beam-scanning applications is discussed in [126]. As shown in Fig.15, the array structure is composed of two LWAs with MTM unit-cells printed on the top surface of the SIW. The MTM unit-cell that is an E-formed transverse slit, leads leakage loss and disconnects the current flow across the SIW to increase the performance parameters of the array. The physical dimension of the LWA is 40 mm × 10 mm × 0.75 mm. The isolation level between the array antennas is boosted through integrating an MTM sheet between the elements. The LWA works throughout the bandwidth of 55 - 65 GHz that corresponds to 16.66% feasible bandwidth. The structure is depicted to display beam-scanning of ±30° across the bandwidth. Backward (−30°), broadside (0°), and forward (+30°) gain are 8.5, 10.1, and 9.5 dBi, respectively. The isolator shield is exhibited to have a minimized influence on the impedance bandwidth and radiation properties. After applying the MTM-sheet an average improvement of ~25 dB, ~1 dBi, and ~13% have been achieved on the isolation, gain, and efficiency, respectively. The surface current density distributions illustrate that the MTM-sheet is an efficient electromagnetic band-gap frame that significantly obstacles surface currents from electromagnetic waves interacting with the closely radiation antennas in the array structure. The ruinous effects of surface currents in the array are remarkably repressed from affecting the array antenna's far-field.

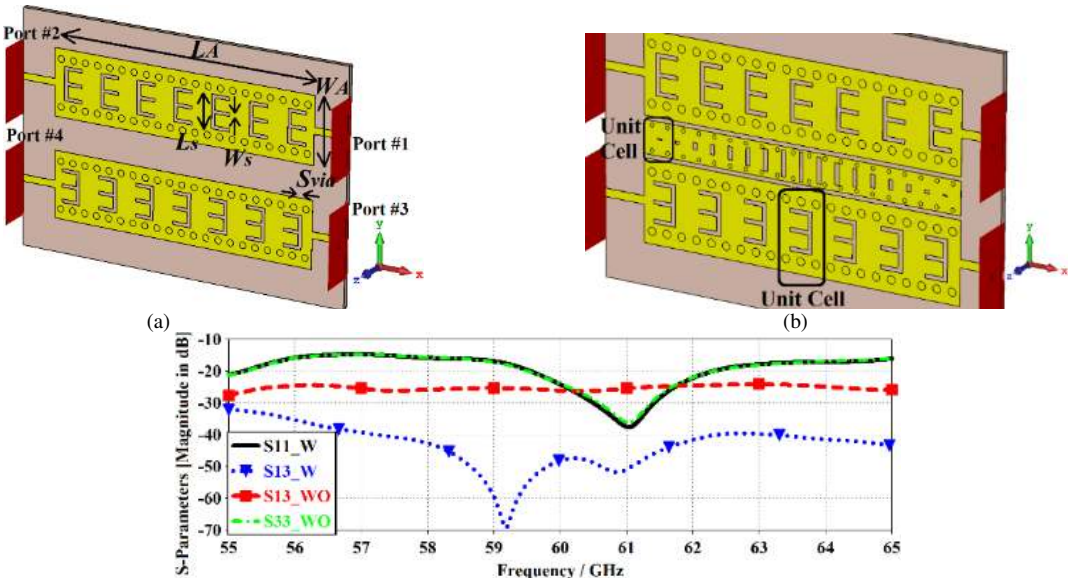

(a) (b)

(c)

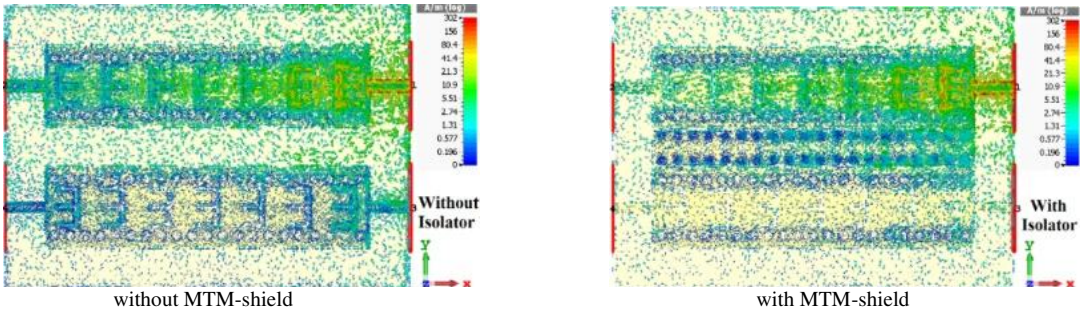

without MTM-shield (d) with MTM-shield

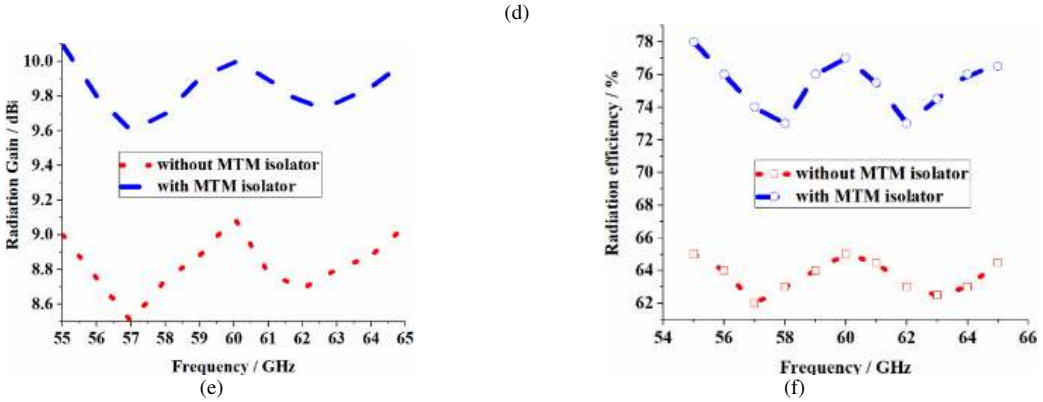

(e) (f)

Fig.15. (a) reference array antenna, (b) proposed antenna array with MTM-shield, (c) S-parameters, (d) surface current density distributions without and with MTM-shield at 60 GHz, (e) gain, and (f) efficiency [126].

F. ISOLATION IMPROVEMENT BETWEEN ANTENNA ARRAYS BASED ON MTS-WALL FOR TERAHERTZ BAND

A new two-dimensional MTS wall to suppress the interference between in antennas in array working at terahertz band of 139 to 141 GHz applicable for security screening, medical and communications systems have been proposed in [127]. The MTS unit-cell contains connected twin 'Y-formed' microstrip structures that are inter-digitally incorporated with each other to generate the MTS wall. The MTS wall does not have via holes, and it includes a shorten ground plane to simplifying the manufacturing process. As shown in Fig.16, the MTS wall is located firmly between the elements to increase the decoupling and suppress the surface-waves. To achieve the lowest coupling, the wall is implemented upright to the antennas. Over the terahertz frequency bandwidth, the gain and isolation of the array antennas are 9.0 dBi and less than -63 dB, respectively. This method obtains isolation improvement of higher than 10dB across a large frequency band (2 GHz) than obtained to date. The decoupling effects are remarked through imagining the surface current curves throughout the array structure. The surface current density distribution shows that without MTS wall and when element #1 is stimulated, the electromagnetic signal is transferred to element #2, and contrariwise. However, when the MTS wall is located between the elements, it remarkably obstructs the electromagnetic signal from element #1 being transferred to element #2. By applying this approach, the edge-to-edge space between the radiation patch has decreased to 2.5mm. The size of the antennas and GND are 5 mm × 5 mm and 9 mm × 4.25 mm when realized on a 1.6 mm thick traditional layer.

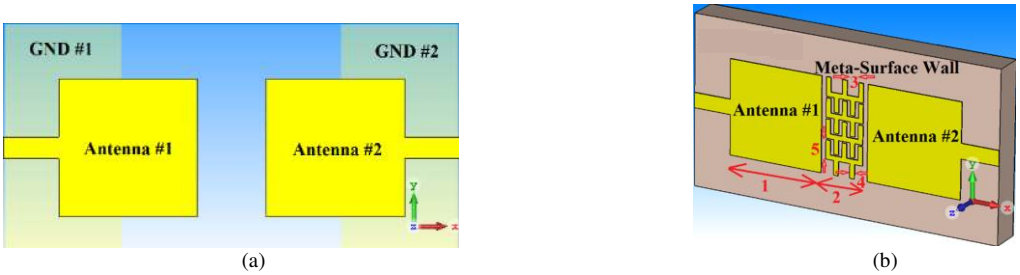

(a) (b)

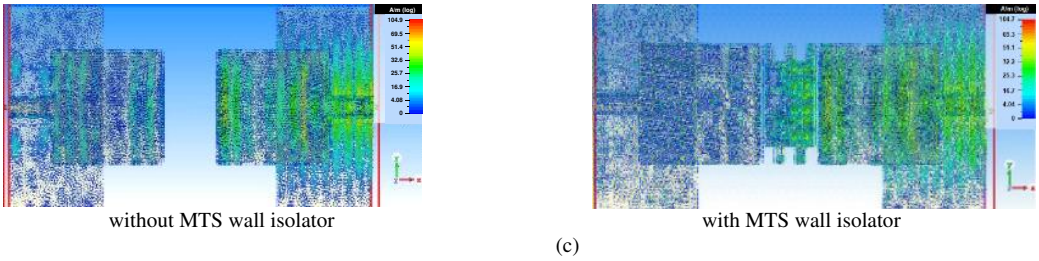

without MTS wall isolator

with MTS wall isolator

(c)

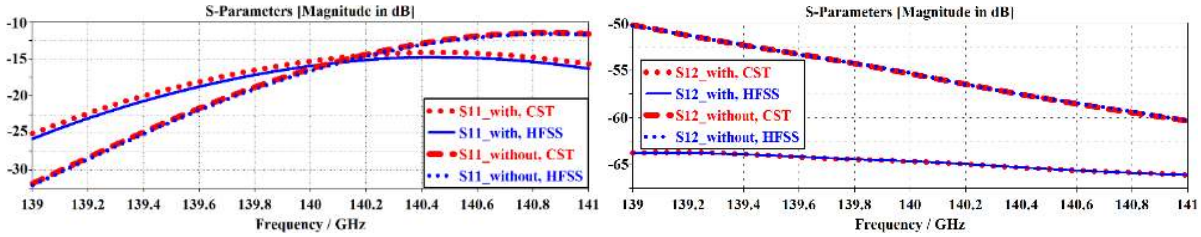

(d)

Fig.16. Antenna array (a) without and (b) with MTS wall isolator, (c) surface current distributions without and with MTS wall isolator at 140 GHz, and (d) S-parameters. [127].

G. ISOLATION IMPROVEMENT ACROSS BROAD FREQUENCY BAND APPLYING INTEGRATED PERIPHERY SLOT FOR ANTENNA ARRAYS

A new mechanism to increase the isolation between closely spaced radiating patches has been proposed and modeled in [128]. This method enabled the implementation of low-profile construction of extremely compact antenna geometries needful in MIMO and SAR communication devices. Contrary to other traditional approaches of reduction interferences where an isolator sheet is placed between the antennas, this method is easier and just needs integrating linear slits close the periphery of the radiating element, as shown in Fig.17. The main properties of this way are (i) substantial suppression in the minimum coupling between the neighbor patches by -26.7dB in X-band and >-15dB in Ku and K-bands; (ii) decrement in the center-to-center distance between the elements up to 10 mm (0.37λ); and (iii) more than 40% gain increment across specified angular directions that changes between 4.5 and 8.2 dBi. The investigation of the surface current distribution shows that the slits act like an isolating frame that soak up the surface-waves that would otherwise couple with the adjacent patches. The proposed technique is easy and inexpensive.

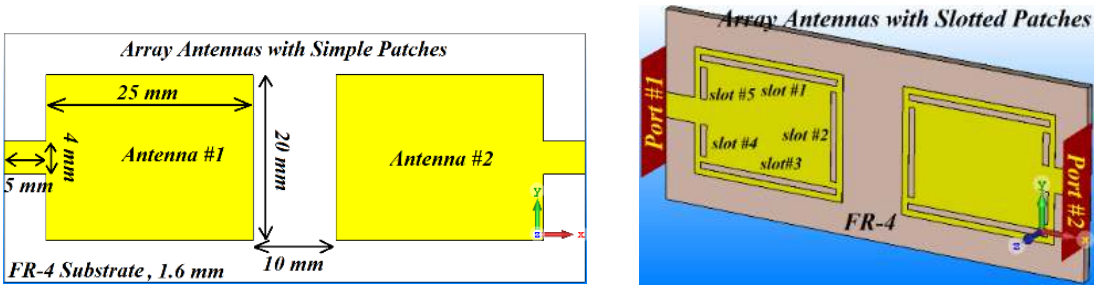

(a) (b)

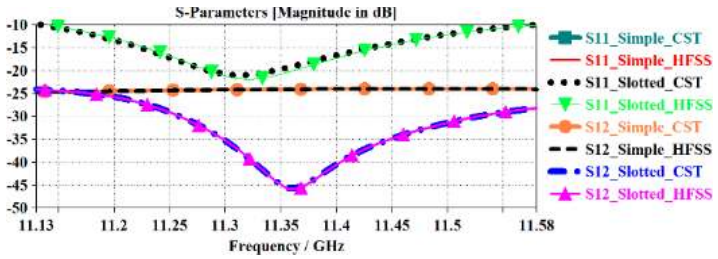

First band

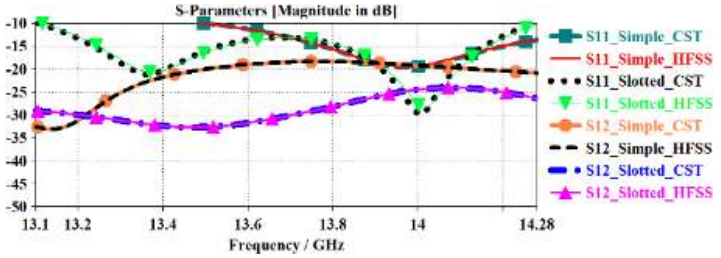

Second band

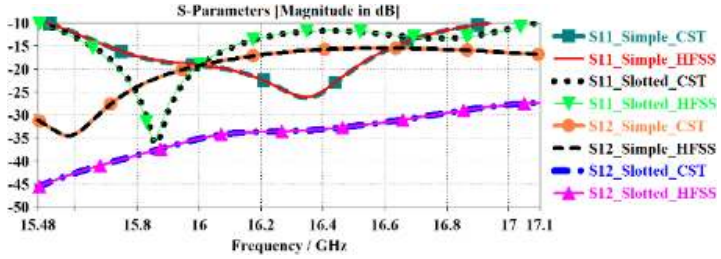

Third band

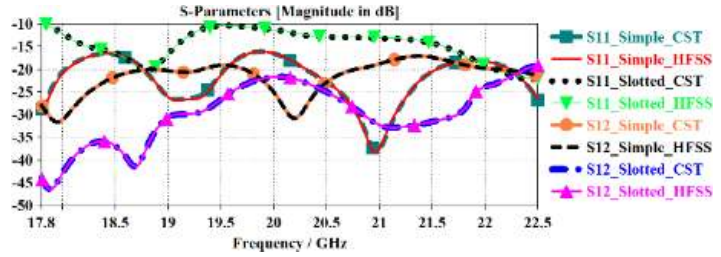

Fourth band

(c)

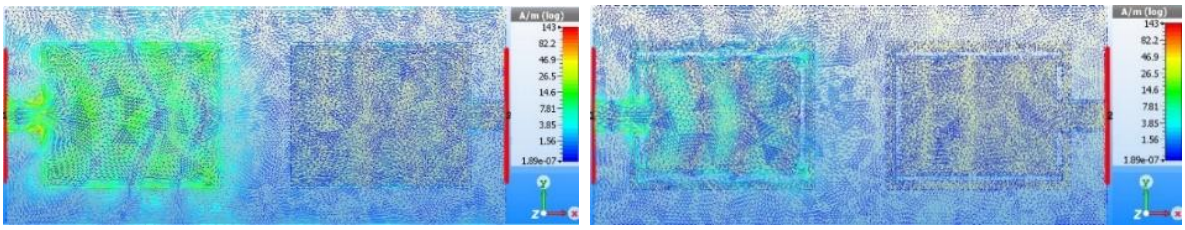

without slotted-patches

with slotted-patches

(d)

Fig.17. (a) Reference array, (b) proposed slotted array, (c) S-parameters, and (d) surface current distributions without and with slotted-patches at 11.37GHz [128].

H. SURFACE-WAVE SUPPRESSION IN ARRAY ANTENNAS APPLYING MTS CONTENT FOR SAR AND MIMO APPLICATIONS

An efficient approach for isolation improvement between closely spaced antennas which is based on MTS decoupling for MIMO and SAR applications, is presented in [132]. It has accomplished by constraining the surface current waves induced across the antenna through the insertion of a cross-formed MTS structure between the antennas, as shown in Fig.18. This MTS minimizes the influences of electromagnetic coupling coming from space-wave and the near-field. Each arm of the cross-formed structure establishing the MTS has a meander-line slit (MLS) etching. The MTS's effectiveness is investigated for a 2×2 antenna array that works throughout six frequency sub-bands in X, Ku, and K-bands. In the X-band, the antenna's applications are wideband global satellite communication systems (WGS) and military communication. In the Ku-band, the antenna's applications are radar and terrestrial microwave, particularly, in police traffic speed-detectors. In the K-band, the antenna's applications are found in airport surface detection equipment (ASDE). Fig.18 illustrates that with this method, the optimum increment obtained in improving isolation between adjacent radiation patches is: 8.5dB (8 to 8.4 GHz), 28dB (9.6 to 10.8 GHz), 27dB (11.7 to 12.6 GHz), 7.5dB (13.4 to 14.2 GHz), 13dB (16.5 to 16.8 GHz) and 22.5dB (18.5 to 20.3 GHz). The results are provided in Table X. Also by employing the presented way, minimal edge-to-edge

space between the elements is achieved up to $0.26\lambda_0$, where λ_0 is specified at 8.0 GHz, the utilize of defected ground plane becomes inessential, apply of via-holes are refrained, the challenge of poor front-to-back ratio is addressed and integration to existing arrays becomes possible.

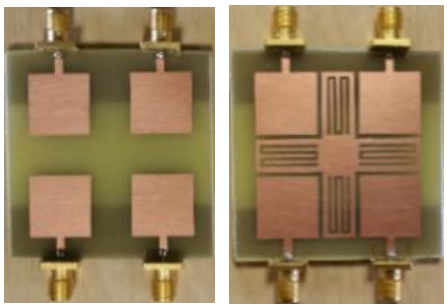

(a)

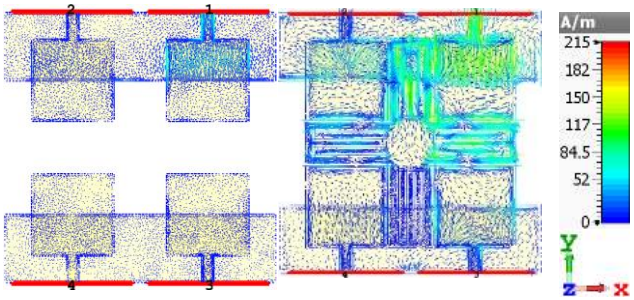

(b)

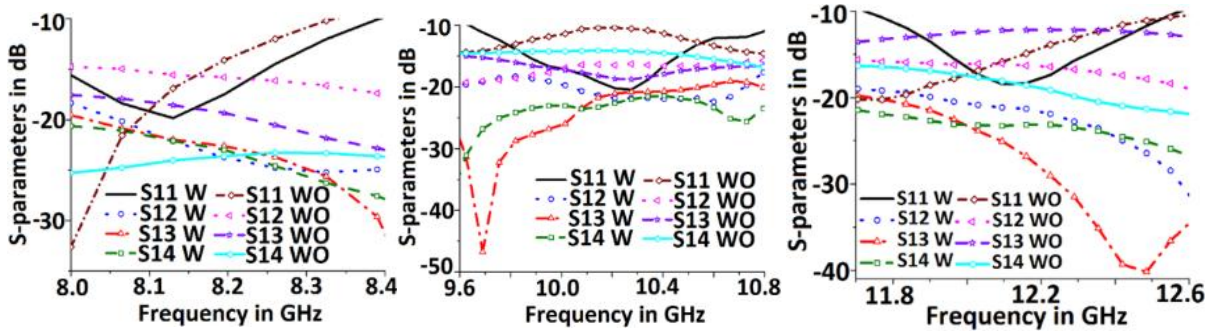

First band Second band Third band

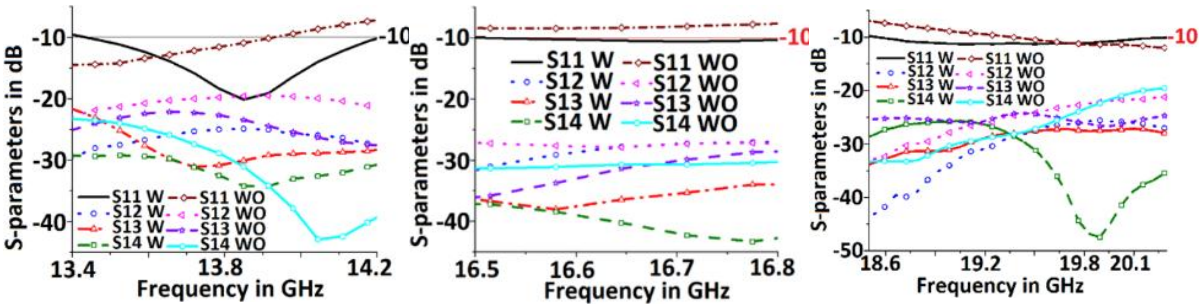

Fourth band Fifth band Sixth band

(c)

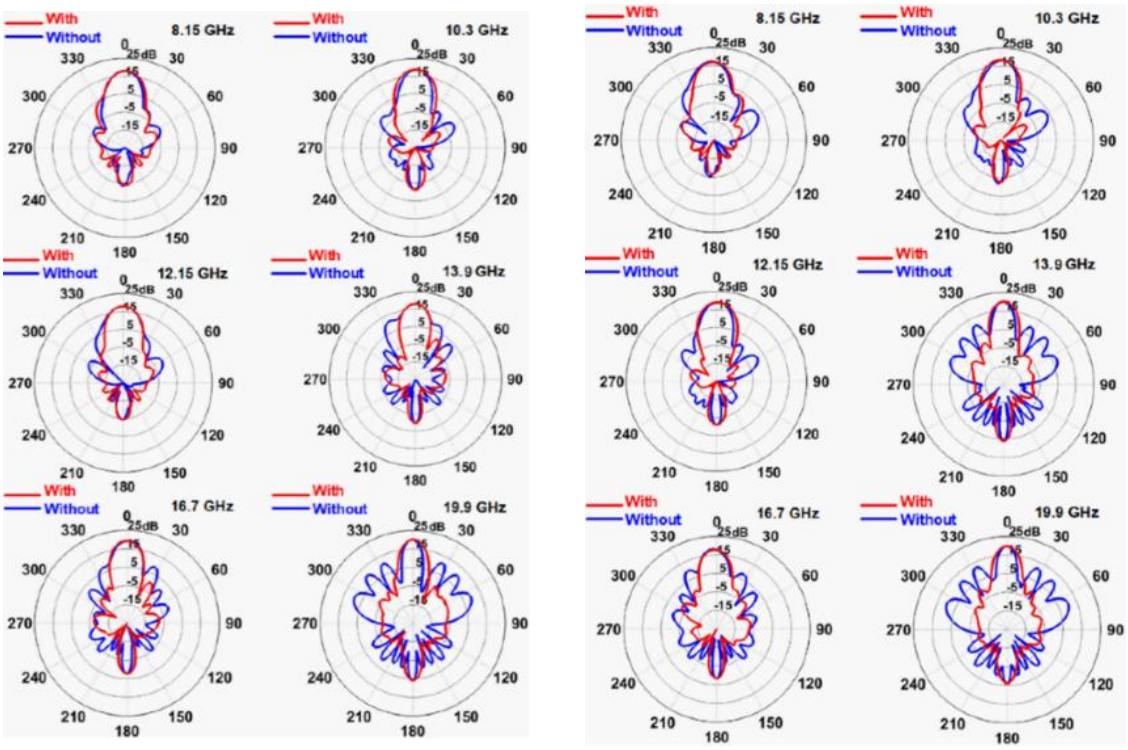

(d)

Fig.18. (a) Manufactured prototypes of the reference and proposed structures before (WO) and after (W) apply MTS decoupling shield, (b) surface current distributions without and with the MTS decoupling shield at 8.15 GHz, (c) measured S-parameters, and (d) measured radiation patterns [132].

TABLE X. ISOLATION IMPROVEMENT WITH METASURFACE

Frequency	$\|S_{12}\|$ () Min., Max., Ave.	$\|S_{13}\|$ (dB) Min., Max., Ave.	$\|S_{14}\|$ (dB) Min., Max., Ave.
I: 8 to 8.4 GHz	7.5 , 8.5 , 8 dB	2 , 8.5 , 6 dB	- , 3 , - dB
II: 9.6 to 10.8 GHz	2.5 , 3.5 , 3 dB	5 , 28 , 17 dB	7 , 18 , 12.5 dB
III: 11.7 to 12.6 GHz	3.5 , 13 , 9.5 dB	8 , 27 , 18 dB	5 , 5 , 5 dB
IV: 13.4 to 14.2 GHz	5.5 , 7.5 , 6.5 dB	- , 4 , 2 dB	- , 6.5 , 3.5 dB
V: 16.5 to 16.8 GHz	- , 3.5 , 2 dB	2 , 5.5 , 4 dB	7 , 13 , 10.5 dB
VI: 18.5 to 20.3 GHz	4.5 , 22.5 , 13.5 dB	2.5 , 7.5 , 5.5 dB	5.5 , 20 , 13 dB

I. STUDY ON INTERFERENCES REDUCTION AND RADIATION BEHAVIOURS OF A 34×34 SIW AND MTS-BASED ARRAY ANTENNAS FOR APPLICATIONS ACROSS 0.125-0.3 THz

In [133], the possibility of a perceptual model of a 34×34 array antenna for working throughout 0.125 to 0.3 THz, which relates to a feasible bandwidth of 82.35% is described. Fig.19 shows that, each of the radiation elements which constitute the array comprises of a square patch having a physical dimension of 2×2 mm^2 and stimulated via a matched microstrip line. Each element has separated from each other by via-holes that are realized based on the SIW method. This approach is exhibited to efficiently improve the isolation between closely spaced antennas that can otherwise disturb the radiation properties. The periphery of each patch is integrated with circular dielectric slits that are implemented based on the MTS principle to improve the radiation performances. By employing these methods, the isolation has improved on average by 25dB across the working bandwidth, and the array's effective aperture area has enlarged with keeping constant its dimensions. The array structure shows a variation on gain and radiation efficiency of 7.51 dBi to 40.08 dBi, and 70.51% to 90.11%, respectively. The data are listed in Table XI. It is clear that after implementing the MTS slits, almost 60% and 30% increments in gain and efficiency have been accomplished. The 34 × 34 antennas array is a suitable candidate to apply in wireless telecommunication apparatus at THz region.

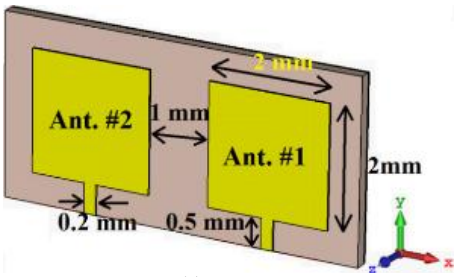

(a)

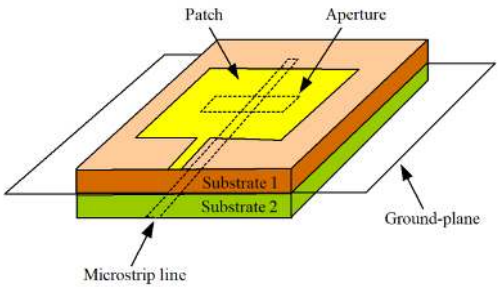

(b)

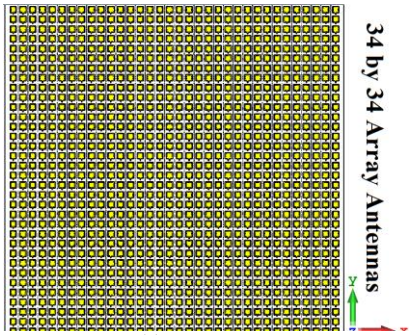

(c)

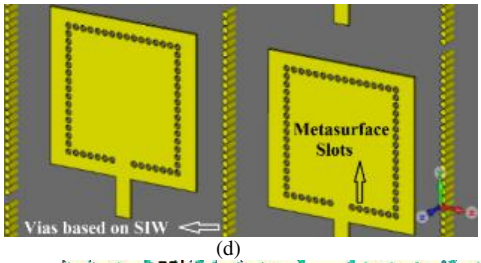

(d)

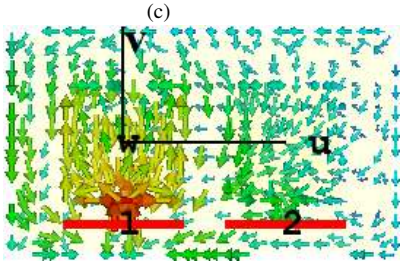

Before employ the SIW and MTS contents

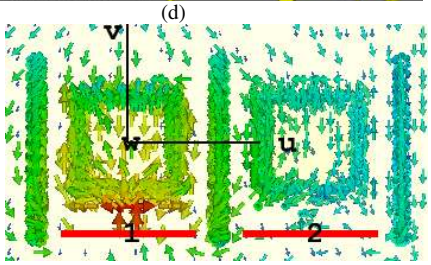

After employ the SIW and MTS contents

(e)

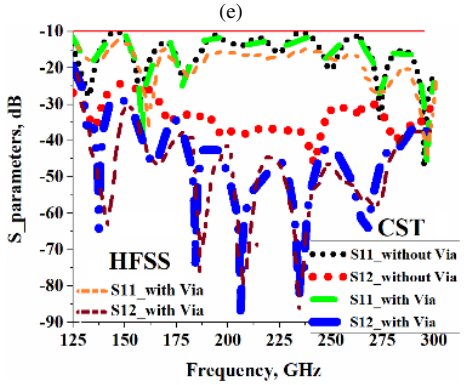

(f)

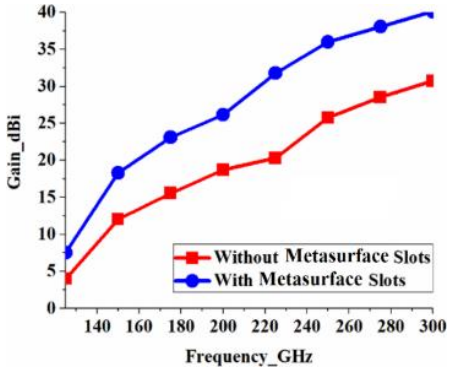

(g)

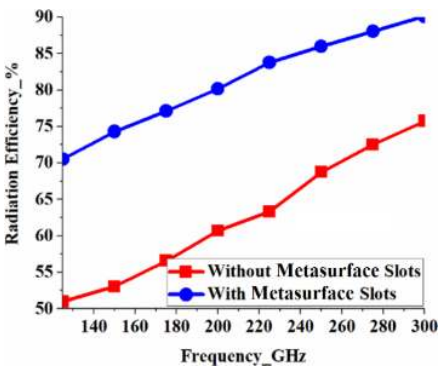

(h)

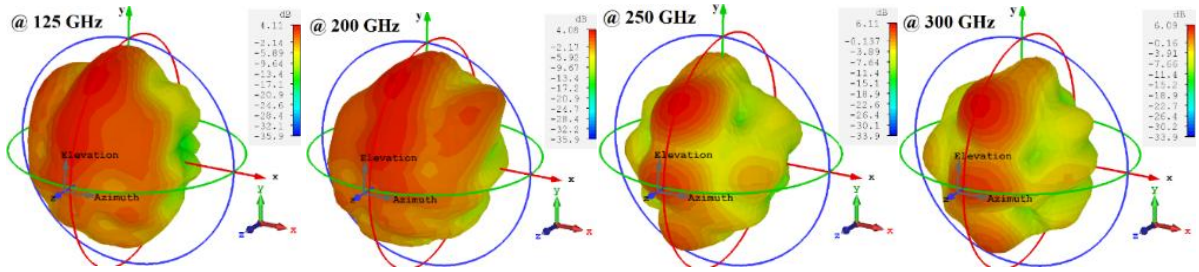

(i)

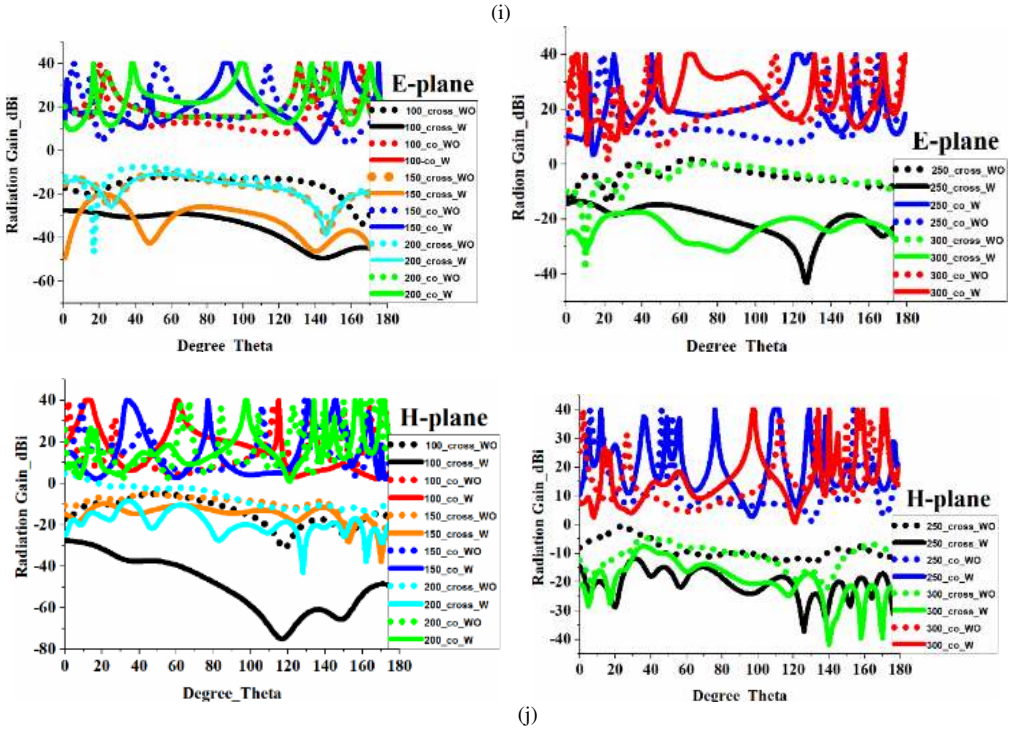

(j)

Fig.19. (a) reference 1×2 array antenna, (b) feeding structure, (c) layout of whole 34×34 array antennas inspired SIW and MTS concepts, (d) zoomed view to depict two central antennas after apply the SIW and MTS principles, (e) surface current density distribution before and after applying the SIW and MTS properties at 250 GHz for two central antennas, (f) S-parameter responses, (g) gain curve, (h) efficiency curve, (i) 3-D radiation diagrams, and (j) co- and cross-polarized radiation gain patterns [133].

TABLE XI. RADIATION PERFORMANCES

	Gain (dBi)
Min. with no metasurface slits	3.96
Min. with metasurface slits	7.51
Improvement	3.55

	Gain (dBi)
Max. with no metasurface slits	30.71
Max. with metasurface slits	40.08
Improvement	9.37

	Efficiency (%)
Min. with no metasurface slits	50.96
Min. with metasurface slits	70.51
Improvement	19.55

	Efficiency (%)
Max. with no metasurface slits	75.71
Max. with metasurface slits	90.11
Improvement	14.40

J. DECOUPLING IMPROVEMENT OF ADJACENT ARRAY ANTENNAS WITH PERIODIC MTM PBG FOR MIMO AND SAR APPLICATIONS

In [134] an MTM photonic bandgap (PBG) periodic structure is utilized as an isolator slab to repress the mutual coupling in densely packed array antenna for SAR and MIMO applications as displayed in Fig.20. By this method, the MTM PBG layout is exhibited to efficiently reduce surface-wave

distributions between the patch arrays by an average of 12dB, see Table XII. MTM PBG layer contains a periodic organization of dielectric circles printed in the cross-formed microstrip sheet that is incorporated between the antennas. It obstacles the distribution of surface-waves on the patches to increment decoupling between the elements. Surface current distribution depicted in Fig.20 provides deeper discernment of how the surface currents are decreased. It is clear that the cross-formed MTM PBG isolator shield dramatically interacts with the surface currents to obstacle them from affecting neighbor antennas in the array configuration. Ruinous influences of surface currents in the antenna are considerably repressed from effecting the antenna array's far-field. The equivalent circuit diagram of the proposed array structure is presented in Fig.20. Contrary to the existing techniques in the literature, the attributes of this method are: (i) easiness; (ii) inexpensive; and (iii) can be retrofitted in available array structures. This structure has fabricated to work across a wide bandwidth of 9.25 to 11 GHz with a feasible bandwidth of 17.28%. By this mechanism (i) the side-lobes have decreased; (ii) there is a negligible influence on the radiation performances; and (iii) the shortest center-to-center distance between neighbor antennas has decreased to 0.15λ at 9.25 GHz. Input impedance calculated utilizing CST software and circuit diagram has been presented in Fig.20. Since the circuit model parameters have extracted applying optimization approach in CST throughout a specific bandwidth, a perfect match between the results achieved by the circuit model and CST has occurred. The gain and efficiency plots have displayed in Fig.20. There is an excellent agreement between the simulated and experimented curves. After apply MTM PBG, a maximum empirical gain and efficiency of 7.85 dBi and 92.78% have obtained at 10.6 GHz. So, before applying the proposed method, the highest magnitude of these parameters was 7.38 dBi and 88.05% at the same frequency. This explains that the radiation specifications are not intensely influenced by realizing the MTM PBG decoupling frame.

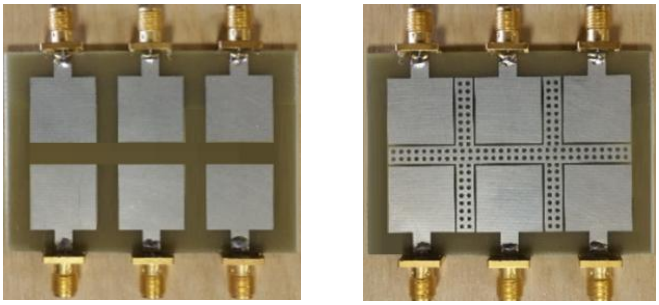

(a) (b)

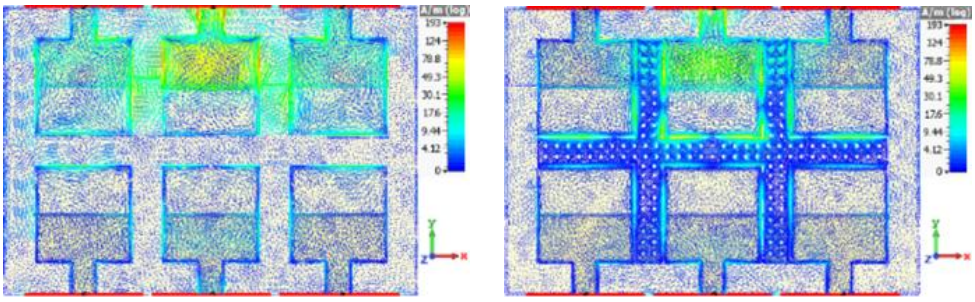

without periodic MTM-PBG isolator with periodic MTM-PBG isolator

(c)

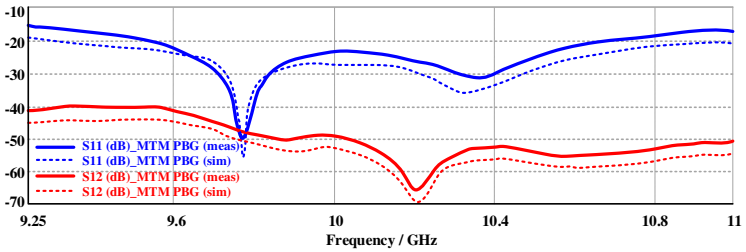

(d)

This article has been accepted for publication in a future issue of this journal, but has not been fully edited. Content may change prior to final publication. Citation information: DOI 10.1109/ACCESS.2020.3032826, IEEE Access

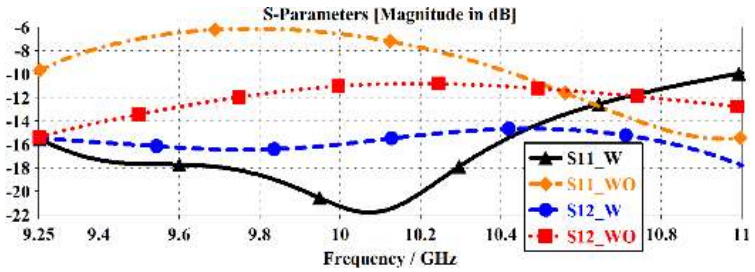

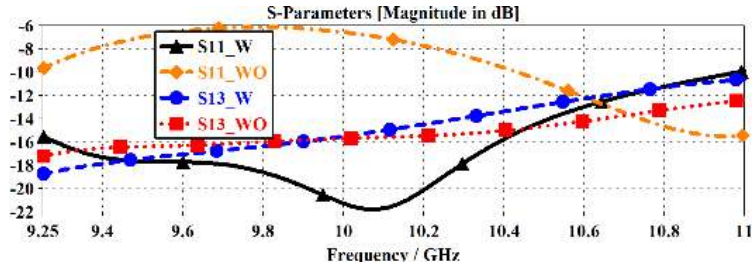

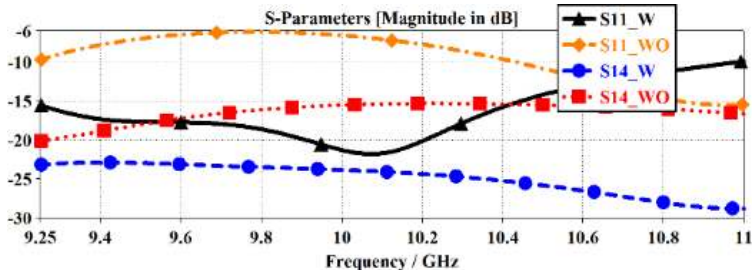

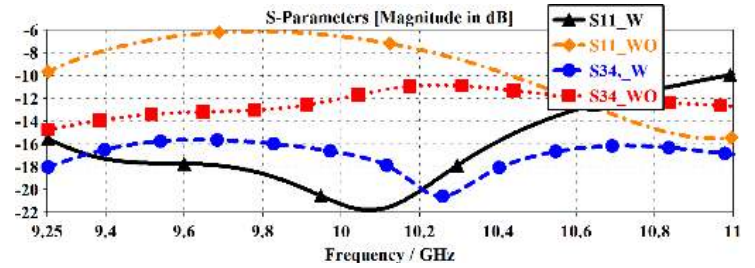

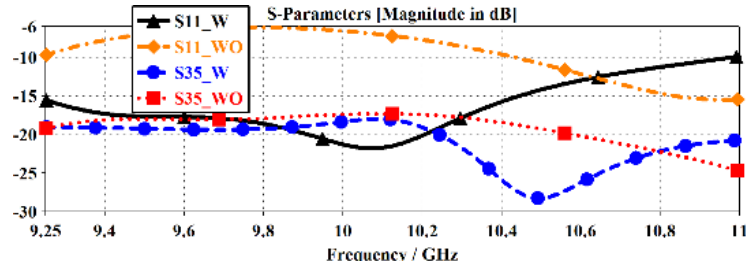

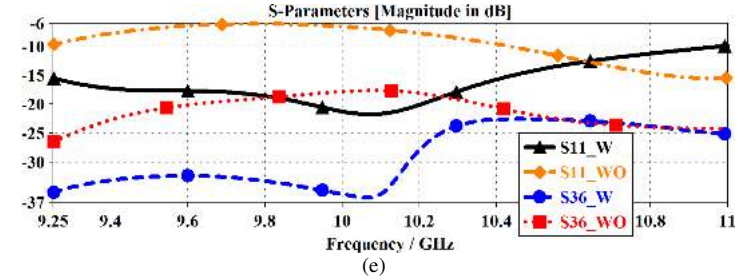

(e)

This article has been accepted for publication in a future issue of this journal, but has not been fully edited. Content may change prior to final publication. Citation information: DOI 10.1109/ACCESS.2020.3032826, IEEE Access

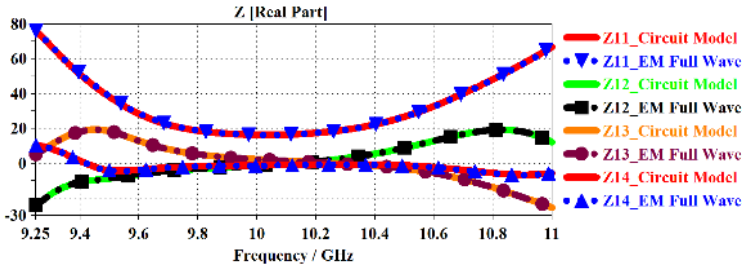

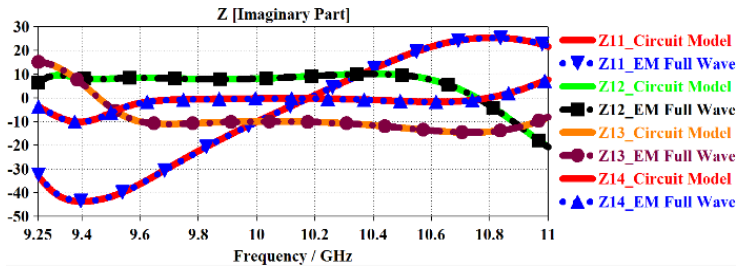

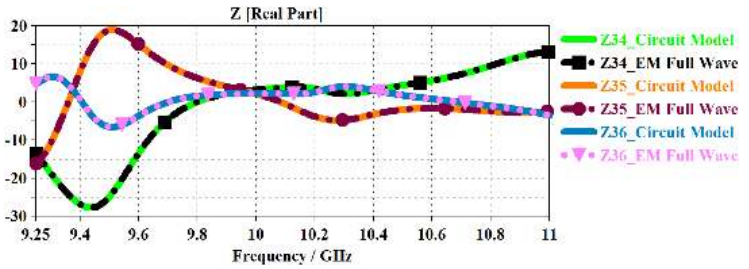

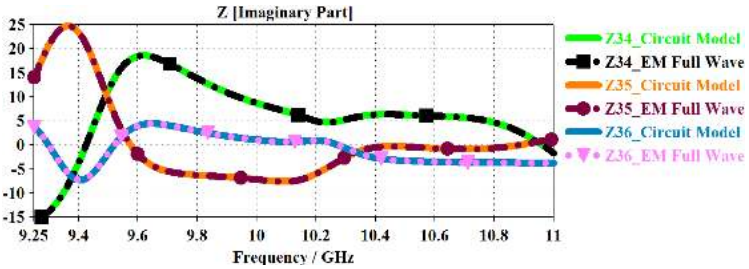

(f)

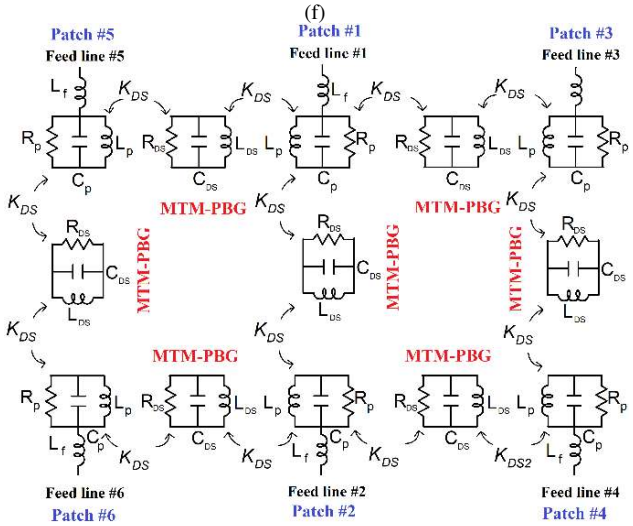

(g)

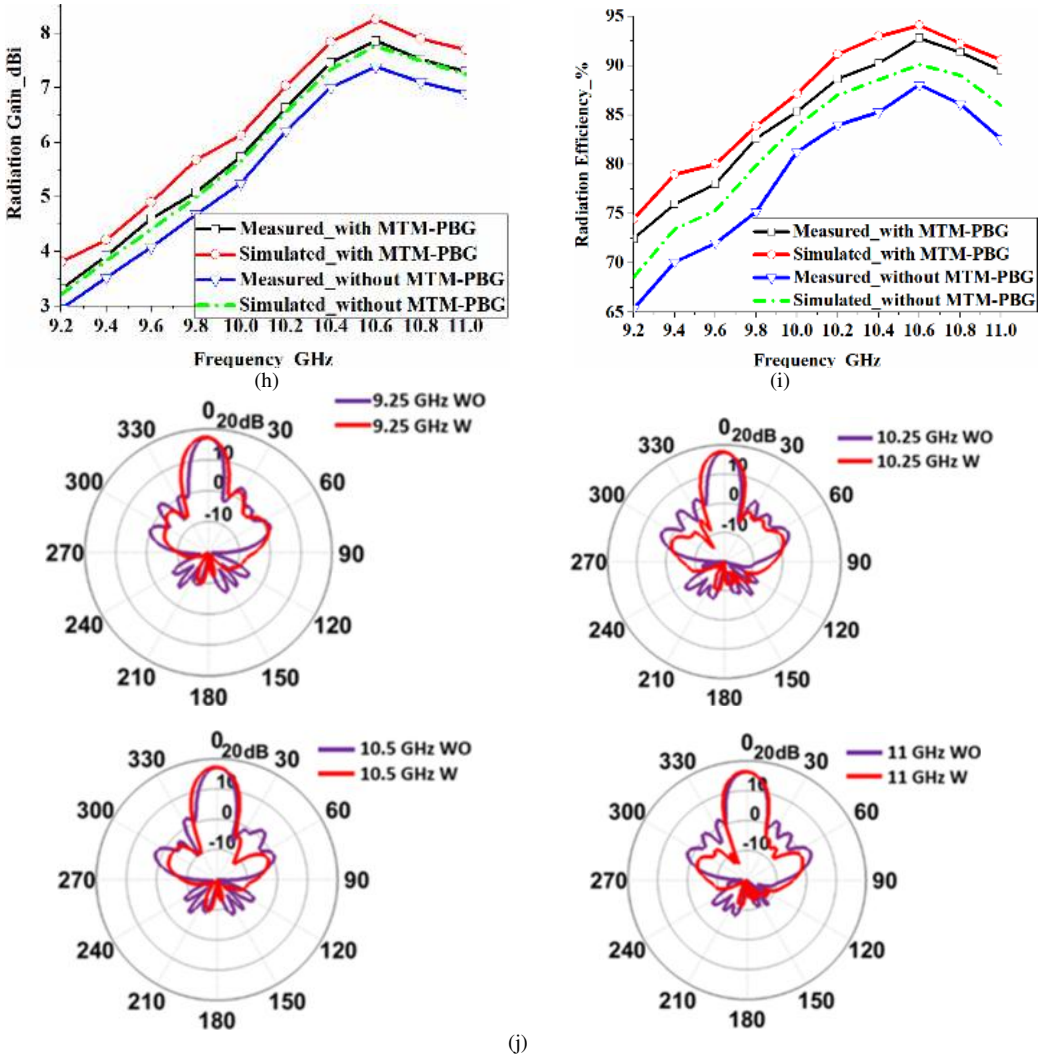

Fig.20. (a) 2×3 reference antenna array, (b) 2×3 proposed antenna array structure with periodic MTM-PBG isolator, (c) surface current distributions without and with periodic MTM-PBG isolator at 9.25 GHz, (d) S-parameters of the MTM PBG isolator, (e) empirical S-parameters of the arrays without (WO) and with (W) proposed isolator, (f) input impedances (Ω) after apply the periodic MTM-PBG isolator, (g) circuit model including MTM-PBG isolator sheet, (h) gain curve, (i) radiation efficiency curve, and (j) experimental radiation patterns before and after the periodic MTM-PBG isolator [134].

TABLE XII. DECOUPLING IMPROVEMENT APPLYING THE PERIODIC MTM PBG TECHNIQUE

S_{11}	9.25 – 11 GHz, FBW = 17.28%	Max. increment of matching: ~15 dB
S_{12} (T/R)	Max. reduction: 5dB @ 10.98 GHz	Ave. reduction: 4dB
S_{13} (T/T)	Max. reduction: 6 dB @9.25GHz	Ave. reduction: 3 dB
S_{14} (T/R)	Max. reduction: 14 dB @ 10.97 GHz	Ave. reduction: 10 dB
S_{34} (T/R)	Max. reduction: 10dB @ 10.25 GHz	Ave. reduction: 8dB
S_{35} (T/T)	Max. reduction: 10dB @ 10.5 GHz	Ave. reduction: 5dB
S_{36} (T/R)	Max. reduction: 19 dB @ 10.07 GHz	Ave. reduction: 7 dB

Table XIII shows comparisons in the performance parameters of the abovementioned techniques relative to the studied literature in terms of the mutual coupling reduction techniques, maximum isolation improvement, number of applied elements in the array structure, design complexity and simplicity, impact on the size after applying the technique, and augmentation and development of the array after applying the technique. Results show that the papers discussed in this section, which are based on combined isolation techniques such as metamaterials, metasurfaces, and EM bandgaps, showcase higher performance parameters with simpler design structures.

TABLE XIII. PERFORMANCE COMPARISON OF DECOUPLING MECHANISMS BASED MIMO AND SAR ANTENNAS

Refs.	Approaches	Max. decoupling improvement (dB)	Number of elements	Symmetricity	Impact on the size after applying the technique	Altering and developing (DGS)	Complexity
[135]	UC-EBG	10	2 (1×2)	NO	Yes	Yes	Yes
[136]	Slot in Ground plane	40	2 (1×2)	NO	Yes	Yes	Yes
[137]	EBG	4	2 (1×2)	NO	Yes	Yes	Yes
[138]	Compact EBG	17	2 (1×2)	NO	Yes	Yes	Yes
[139]	DGS	17.43	2 (1×2)	NO	Yes	Yes	Yes
[140]	U-shaped resonator	10	2 (1×2)	NO	Yes	Yes	Yes
[141]	Slotted Meander Line Resonator	16	2 (1×2)	NO	Yes	Yes	Yes
[142]	I-shaped resonator	30	2 (1×2)	NO	Yes	Yes	Yes
[143]	SCSRR	10	2 (1×2)	NO	Yes	Yes	Yes
[144]	SCSSRR	14.6	2 (1×2)	NO	Yes	Yes	Yes
[145]	Waveguide MTM	20	2 (1×2)	NO	Yes	Yes	Yes
[146]	Waveguide MTM	18	2 (1×2)	NO	Yes	Yes	Yes
[147]	Meander line resonator	10	2 (1×2)	NO	Yes	Yes	Yes
[148]	Fractal load with DGS	16	2 (1×2)	NO	Yes	Yes	Yes
[149]	Antenna Interference Cancellation Chip (AICC)	15	2 (1×2)	Yes	No	No	Yes
[150]	3-D Metamaterial Structure (3DMMS)	18	2 (1×2)	Yes	Yes	No	No
[122]	Metamaterial fractal load	37	2 (1×2)	Yes	NO	NO	NO
[123]	Fractal metamaterial electromagnetic bandgap	17 for S_{12} 37 for S_{13} 17 for S_{14}	4 (2×2)	Yes	NO	NO	NO
[124]	Metamaterial	57	2 (1×2)	Yes	NO	NO	NO
[125]	Metamaterial	40 for S_{12} ~7 for S_{13} 11 for S_{14}	4 (2×2)	Yes	NO	NO	NO
[126]	Metamaterials and Substrate Integrated Waveguide	42.5	2 (2×1)	Yes	NO	NO	NO
[127]	Metasurface wall isolator	13.5	2 (1×2)	Yes	NO	NO	NO
[128]	Slots	>26	2 (1×2)	Yes	NO	NO	NO
[132]	Metasurface	32 (X-band) 27 (Ku-band) 26 (K-band)	4 (2×2)	Yes	NO	NO	NO
[133]	SIW & Metasurface	50	1156 (34×34)	Yes	NO	NO	NO
[134]	MTM-PBG	10 for S_{34} 14 for S_{14} 19 for S_{36}	6 (3×2)	Yes	NO	NO	NO

VI. CONCLUSION

Antenna arrays plays an important role in improving various radiation characteristics of antennas. The mutual coupling between radiation elements in the array is an undesirable effect which degrades the performance of array. Over the years many compensation techniques have been proposed to overcome such harmful effects. The effectiveness of various methods mainly depends on the applications in which arrays are to be implemented. The survey presented here provides a comprehensive study on the investigations on various isolation improvement approaches based on metamaterial and metasurface inspired techniques for antenna arrays. It is well known that strong mutual coupling tends to occur between antenna elements that are closely spaced to each other as in the case of antenna arrays where the average element spacing is smaller than about half a wavelength. The consequence of strong mutual coupling is distortion in the array's performance, and it constrains the array's miniaturization. Therefore, in the multiple-input multiple-output (MIMO) and synthetic aperture radar (SAR) systems, high isolation is very important. In SAR systems the coupling effect is also known to influence the resolution capability, interference rejection, and direction-of-arrival (DOA) estimation.

Mutual coupling reduction is an important area of research which has direct impact on the development of the next generation wireless communication systems, such as 5G, 6G and massive MIMO. Although several isolation improvement approaches are reported in the literature to date, most of these studies are confined to two-port antenna arrays. This

review discusses diverse and promising decoupling methods based on metamaterial/metasurface inspired techniques for applications such as MIMO and SAR systems. Comprehensive comparisons are given of the various techniques and how they affect the radiation performance of the arrays. The main aim of researchers is to mitigate or suppress the mutual coupling as much as possible with negligible effect on the array's performance and, if possible, without increasing the array's physical footprint. To achieve this aim researchers have employed various techniques including the use of complementary split-ring resonators (CSRR) and defected ground structures (DGS). This review should serve as a reference for researchers to advance the art.

ACKNOWLEDGMENTS

This work is partially supported by RTI2018-095499-B-C31, Funded by Ministerio de Ciencia, Innovación y Universidades, Gobierno de España (MCIU/AEI/FEDER,UE), and innovation programme under grant agreement H2020-MSCA-ITN-2016 SECRET-722424 and the financial support from the UK Engineering and Physical Sciences Research Council (EPSRC) under grant EP/E022936/1.

REFERENCES

[1] M. Sánchez-Fernández, et. al., "Spectral efficiency in MIMO systems using space and pattern diversities under compactness constraints," IEEE Trans. Veh. Technol., vol. 57, no. 3, pp. 1637-1645, May 2008.
[2] L. Wang, et. al., "Suppressing mutual coupling of MIMO antennas with parasitic fragment-type elements," in Proc. 46th Eur. Microw. Conf. (EuMC), 2016, pp. 1303-1306.
[3] X. Wang, et al., "Pattern and polarization diversity antenna with high isolation for portable wireless devices," IEEE Antennas Wireless Propag. Lett., vol. 8, pp. 209-211, 2009.
[4] A. J. Paulraj, et al., "An overview of MIMO communications-A key to gigabit wireless," Proc. IEEE, vol. 92, no. 2, pp. 198-218, Feb. 2004.
[5] K. Wei, et al., "Microstrip antenna array mutual coupling suppression using coupled polarisation transformer," IET Microw., Antennas Propag., vol. 11, no. 13, pp. 1836-1840, Jul. 2017.
[6] L. H. Trinh, et al., "4×4 MIMO multiband antenna system for mobile handsets," Int. J. Antennas Propag., vol. 2015, Nov. 2015, Art. no. 857876.
[7] Z. Ying, "Antennas in cellular phones for mobile communications," Proc. IEEE, vol. 100, no. 7, pp. 2286-2296, Jul. 2012.
[8] P.-Y. Qin, et al., "Effect of antenna polarization diversity on MIMO system capacity," IEEE Antennas Wireless Propag. Lett., vol. 9, pp. 1092-1095, Nov. 2010.
[9] H. S. Lui and H. T. Hui, "Mutual coupling compensation for direction-of arrival estimations using the receiving-mutual-impedance method," Int. J. Antennas Propag., vol. 2010, Jan. 2010, Art. no. 373061.
[10] Y. Wu, et al., "Effects of antenna correlation and mutual coupling on the carrier frequency offset estimation in MIMO systems," in Proc. 6th Int. Conf. Wireless Commun. Netw. Mobile Comput. (WiCOM), 2010, pp. 1-4.
[11] B. Wang, et al., "Performance of the large-scale adaptive array antennas in the presence of mutual coupling," IEEE Trans. Antennas Propag., vol. 64, no. 6, pp. 2236-2245, Jun. 2016.
[12] D. M. Pozar, "A relation between the active input impedance and the active element pattern of a phased array," IEEE Trans. Antennas Propag., vol. 51, no. 9, pp. 2486-2489, Sep. 2003.
[13] Iram Nadeem, and Dong-You Choi, "Study on Mutual Coupling Reduction Technique for MIMO Antennas", IEEE Access, Volume 7, pp. 563 – 586, 2019.
[14] X. Chen, et al., "A review of mutual coupling in MIMO systems," IEEE Access, vol. 6, pp. 24706-24719, 2018.
[15] H. Singh, et al., "Mutual coupling in phased arrays: A review," Int. J. Antennas Propag., vol. 2013, Mar. 2013, Art. no. 348123.
[16] C. Craeye and D. González-Ovejero, "A review on array mutual coupling analysis," Radio Sci., vol. 46, no. 2, pp. 1-25, 2011.
[17] X. Zhu, et al., "Compact UWB-MIMO antenna with metamaterial FSS decoupling structure," J. Wireless Commun. Netw., vol. 2017, no. 1, p. 115, Dec. 2017.
[18] Y. Ou, et al., "Two-element compact antennas decoupled with a simple neutralization line," Prog. Electromagn. Res., vol. 65, pp. 63-68, 2017.
[19] C.H. See, R.A. Abd-Alhameed, Z.Z. Abidin, N.J. McEwan and P.S. Excell, "Wideband Printed MIMO/Diversity Monopole Antenna for WiFi/WiMAX Applications," IEEE Trans. Antennas and Propagation, vol.60, no.4, pp.2028-2035, April 2012.
[20] C.H. See, H.I. Hraga, J.M. Noras, R.A. Abd-Alhameed and N.J. McEwan, "Compact Multiple Input and Multiple Output/Diversity Antenna for Portable and Mobile Ultra-wideband applications," IET Microwaves, Antennas & Propagation, vol. 7, pp.444-451, April 2013.
[21] M. Bilal, et al., "An FSS-based nonplanar quad-element UWB-MIMO antenna system," IEEE Antennas Wireless Propag. Lett., vol. 16, pp. 987-990, 2017.
[22] M. S. Khan, et al., "A compact CSRR-enabled UWB diversity antenna," IEEE Antennas Wireless Propag. Lett., vol. 16, pp. 808-812, 2017.
[23] M. A. Abdalla and A. A. Ibrahim, "Design and performance evaluation of metamaterial inspired MIMO antennas for wireless applications," Wireless Pers. Commun., vol. 95, no. 2, pp. 1001-1017, 2017.
[24] Y.-S. Chen and C.-P. Chang, "Design of a four-element multiple-input multiple-output antenna for compact long-term evolution small-cell base stations," IET Microw., Antennas Propag., vol. 10, no. 4, pp. 385-392, 2016.
[25] C.H. See, R.A. Abd-Alhameed, N.J. McEwan, S.M.R. Jones, R Asif and P.S. Excell, "Design of Printed MIMO/Diversity Monopole Antenna for Future Generation Handheld Devices," International Journal of RF and Microw. Computer-Aided Engineering, vol.24, no.3, pp.348-359, May 2014.
[26] Wang, Z., Zhao, L., Cai, Y. et al. A Meta-Surface Antenna Array Decoupling (MAAD) Method for Mutual Coupling Reduction in a MIMO Antenna System. Sci Rep **8,** 3152 (2018). https://doi.org/10.1038/s41598-018-21619-z.
[27] J. Tang *et al*., "A Metasurface Superstrate for Mutual Coupling Reduction of Large Antenna Arrays," *IEEE Access*, vol. 8, pp. 126859-126867, 2020, doi: 10.1109/ACCESS.2020.3008162.
[28] K. Wu, C. Wei, X. Mei and Z. Zhang, "Array-Antenna Decoupling Surface," *IEEE Transactions on Antennas and Propagation*, vol. 65, no. 12, pp. 6728-6738, Dec. 2017, doi: 10.1109/TAP.2017.2712818.
[29] M. Li, X. Chen, A. Zhang, W. Fan and A. A. Kishk, "Split-Ring Resonator-Loaded Baffles for Decoupling of Dual-Polarized Base Station Array," *IEEE Antennas and Wireless Propagation Letters*, vol. 19, no. 10, pp. 1828-1832, Oct. 2020.
[30] S. Chouhan, et. al., "Multiport MIMO antennas with mutual coupling reduction techniques for modern wireless transreceive operations: A review," Int. J. RF Microw. Comput.-Aided Eng., vol. 28, no. 2, pp. 1-13, Feb. 2018.
[31] A. Dadgarpour, et al., "Mutual coupling reduction in dielectric resonator antennas using metasurface shield for 60-GHz MIMO systems," IEEE Antennas Wireless Propag. Lett., vol. 16, pp. 477_480, 2017.
[32] G. Zhai, et al., "Enhanced isolation of a closely spaced four-element MIMO antenna system using metamaterial mushroom," IEEE Trans. Antennas Propag., vol. 63, no. 8, pp. 3362_3370, Aug. 2015.
[33] M. Akbari, et.al., "Spatially decoupling of CP antennas based on FSS for 30-GHz MIMO systems," IEEE Access, vol. 5, pp. 6527_6537, 2017.

[34] R. Karimian, et al., "Low-mutual coupling 60-GHz MIMO antenna system with frequency selective surface wall," IEEE Antennas Wireless Propag. Lett., vol. 16, pp. 373-376, 2017.
[35] S. Shrestha, et al., "Comparative study of antenna designs for RF energy harvesting," Int. J. Antennas Propag., vol. 2013, Jan. 2013, Art. no. 385260.
[36] M. S. Sharawi, et al., "Correlation coefficient calculations for MIMO antenna systems: A comparative study," Int. J. Microw. Wireless Technol., vol. 9, no. 10, pp. 1991-2004, 2017.
[37] L. Malviya, et al., "MIMO antennas with diversity and mutual coupling reduction techniques: A review," Int. J. Microw. Wireless Technol., vol. 9, no. 8, pp. 1763-1780, 2017.
[38] L. Savy and M. Lesturgie, "Coupling effects in MIMO phased array," Proc. IEEE Radar Conf., Philadelphia, PA, USA, May 2016, pp. 1-6.
[39] L. K. Yeung and Y. E. Wang, "Mode-based beamforming arrays for miniaturized platforms," IEEE Trans. Microw. Theory Techn., vol. 57, no. 1, pp. 45_52, Jan. 2009.
[40] J. Andersen and H. Rasmussen, "Decoupling and descattering networks for antennas," IEEE Trans. Antennas Propag., vol. AP-24, no. 6, pp. 841_846, Nov. 1976.
[41] L. Zhao, et al., ``A novel second-order decoupling network for two-element compact antenna arrays," in Proc. Asia_Paci_c Microw. Conf., 2012, pp. 1172_1174.
[42] K.-L. Wong, et al., "Two asymmetrically mirrored gap-coupled loop antennas as a compact building block for eight-antenna MIMO array in the future smartphone," IEEE Trans. Antennas Propag., vol. 65, no. 4, pp. 1765_1778, Apr. 2017.
[43] B. K. Lau, et al., "Impact of matching network on bandwidth of compact antenna arrays," IEEE Trans. Antennas Propag., vol. 54, no. 11, pp. 3225_3238, Nov. 2006.
[44] L. Zhao, et al., "A coupled resonator decoupling network for two-element compact antenna arrays in mobile terminals," IEEE Trans. Antennas Propag., vol. 62, no. 5, pp. 2767_2776, May 2014.
[45] Mak ACK, et al., "Isolation enhancement between two closely packed antennas," IEEE Trans. Antenna Propag. 2008; 56: 3411–3419.
[46] Chen S, et al., "A decoupling technique for increasing the port isolation between two strongly coupled antennas," IEEE Trans Antenna Propag. 2008; 56: 3650–3658.
[47] Baek J, Choi J., "The design of a LTE/MIMO antenna with high isolation using a decoupling network," Microwave Opt Technol Lett. 2014; 56: 2187–2190.
[48] Choukiker YK, et al., "Hybrid fractal shape planar monopole antenna covering multiband wireless communications with MIMO implementation for handheld mobile devices," IEEE Trans Antenna Propag. 2014; 62: 1483–1488.
[49] Kewei Q, Decheng G, "Compact tunable network for closely spaced antennas with high isolation," Microwave Opt Technol Lett. 2016; 58: 65–69.
[50] Li Z, et al., "Compact dual-band MIMO antenna for 4G USB dongle applications," Microwave Opt. Technol. Lett. 2012; 54: 744–748.
[51] Lee W, Jang B, "A small 4 by 4 MIMO antenna system for LTE smart phones," Microwave Opt. Technol. Lett. 2016;58: 2668–2672.
[52] Liu Y, et al., "Dual-band planar MIMO antenna for WLAN application," Microwave Opt. Technol. Lett. 2015; 57: 2257–2262.
[53] Yu Y, et al., "A compact MIMO antenna with improved isolation bandwidth for mobile applications," Microwave Opt. Technol. Lett. 2011; 53: 2314–2317.
[54] Park B, et al., "Design of a decoupled MIMO antenna for LTE applications," Microwave Opt. Technol. Lett. 2011; 53: 582–586.
[55] Bilal M, et al., "MIMO application UWB antenna doublet incorporating a sinusoidal decoupling structure," Microwave Opt. Technol. Lett. 2014; 56: 1547–1553.
[56] D. Wu, et. al., "Decoupling using diamond-shaped patterned ground resonator for small MIMO antennas," IET Microw., Antennas Propag., vol. 11, no. 2, pp. 177-183, 2017.
[57] L. Zhao and K.-L. Wu, "A decoupling technique for four-element symmetric arrays with reactively loaded dummy elements," IEEE Trans. Antennas Propag., vol. 62, no. 8, pp. 4416-4421, Aug. 2014.
[58] L. Zhao and K.-L. Wu, "A dual-band coupled resonator decoupling network for two coupled antennas," IEEE Trans. Antennas Propag., vol. 63, no. 7, pp. 2843_2850, Jul. 2015.
[59] C. F. Ding, et al., "Novel pattern-diversity-based decoupling method and its application to multielement MIMO antenna," IEEE Trans. Antennas Propag., vol. 66, no. 10, pp. 4976_4985, Oct. 2018.
[60] C.-X. Mao and Q.-X. Chu, "Compact coradiator UWB-MIMO antenna with dual polarization," IEEE Trans. Antennas Propag., vol. 62, no. 9, pp. 4474-4480, Sep. 2014.
[61] S. T. Fan, et al., "Bandwidth enhancement of a printed slot antenna with a pair of parasitic patches," IEEE Antennas Wireless Propag. Lett., vol. 11, pp. 1230-1233, 2012.
[62] J. S. Row and S. W. Wu, "Circularly-polarized wide slot antenna loaded with a parasitic patch," IEEE Trans. Antennas Propag., vol. 56, no. 9, pp. 2826-2832, Sep. 2008.
[63] Li Z, et al., "Reducing mutual coupling of MIMO antennas with parasitic elements for mobile terminals," IEEE Trans Antenna Propag. 2012; 60: 473–481.
[64] Ayatollahi M, et al., "A compact high isolation and wide bandwidth antenna array for long term evolution wireless devices," IEEE Trans Antenna Propag. 2012;60:4960–4963.
[65] Soltani S, Murch RD, "A compact planar printed MIMO antenna design," IEEE Trans Antenna Propag. 2015; 63: 1140–1149.
[66] R. V. S. R. Krishna and R. Kumar, "Microstrip fed square ring slot antenna for ultra-wideband dual polarisation with good isolation," IET Microw., Antennas Propag., vol. 10, no. 7, pp. 791_796, 2016.
[67] T. K. Roshna, et al., "A compact UWB MIMO antenna with re_ector to enhance isolation," IEEE Trans. Antennas Propag., vol. 63, no. 4, pp. 1873-1877, Apr. 2015.
[68] S. Zhang, et al., "Ultrawideband MIMO/diversity antennas with a tree-like structure to enhance wideband isolation," IEEE Antennas Wireless Propag. Lett., vol. 8, pp. 1279-1282, 2009.
[69] G. Srivastava and A. Mohan, "Compact MIMO Slot antenna for UWB applications," IEEE Antennas Wireless Propag. Lett., vol. 15, pp. 1057-1060, 2016.
[70] M. S. Khan, et al., "Ultra-compact dual-polarised UWB MIMO antenna with meandered feeding lines," IET Microw., Antennas Propag., vol. 11, no. 7, pp. 997-1002, 2017.
[71] M. K. Khandelwal, et al., "Defected ground structure: Fundamentals, analysis, and applications in modern wireless trends," Int. J. Antennas Propag., vol. 2017, Feb. 2017, Art. no. 2018527.
[72] A. K. Arya, et al., "Defected ground structure in the perspective of microstrip antennas: A review," Frequenz, vol. 64, pp. 79-84, Jun. 2010.
[73] P. Lindberg, et al., "Technique of ground size tuning for isolation between monopoles in compact wireless terminals," IEEE Trans Antenna Propag. 2012; 60: 5488–5491.
[74] Lu J, et al., "A high-isolation dual-polarization microstrip patch antenna with quasi-cross-shaped coupling slot," IEEE Trans Antenna Propag. 2011; 59: 2713–2717.
[75] R. Hussain, et al., "Planar meandered F-shaped 4-element reconfigurable multiple-input–multiple output antenna system with isolation enhancement for cognitive radio platforms," IET Microwaves Antennas Propag., 2016; 10: 45–52.
[76] K. Wei, et al., "S-shaped periodic defected ground structures to reduce microstrip antenna array mutual coupling," Electron. Lett., vol. 52, no. 15, pp. 1288_1290, 2016.
[77] R. Anitha, et al., "Enhanced isolation with defected ground structure in MIMO antenna,"' Electron. Lett., vol. 50, no. 24, pp. 1784-1786, 2014.
[78] C. R. Jetti and V. R. Nandanavanam, "Trident-shape strip loaded dual band-notched UWB MIMO antenna for portable device applications," AEU-Int. J. Electron. Commun., vol. 83, pp. 11-21, Jan. 2018.
[79] F. G. Zhu, et al., "Reduction of mutual coupling between closely-packed antenna elements using defected ground structure," Electron. Lett., vol. 45, no. 12, pp. 601-602, Jun. 2009.
[80] A. Ramachandran, et al., "A four-port MIMO antenna using concentric square-ring patches loaded with CSRR for high isolation," IEEE Antennas Wireless Propag. Lett., vol. 15, pp. 1196-1199, 2016.

[81] M. S. Sharawi, et al., "A CSRR loaded MIMO antenna system for ISM band operation," IEEE Trans. Antennas Propag., vol. 61, no. 8, pp. 4265-4274, Aug. 2013.
[82] D.-G. Yang, et al., "Design of dual-band MIMO monopole antenna with high isolation using slotted CSRR for WLAN," Microw. Opt. Technol. Lett., vol. 56, no. 10, pp. 2252-2257, 2014.
[83] P. R. Prajapati, "Application of defected ground structure to suppress outof- band harmonics for WLAN microstrip antenna," Int. J. Microw. Sci. Technol., vol. 2015, Nov. 2015, Art. no. 210608.
[84] Y. Wang and Z. Du, "A wideband printed dual-antenna with three neutralization lines for mobile terminals," IEEE Trans. Antennas Propag., vol. 62, no. 3, pp. 1495-1500, Mar. 2014.
[85] Su S, Lee C, Chang F, "Printed MIMO-antenna system using neutralization-line technique for wireless USB-dongle applications," IEEE Trans Antenna Propag. 2012; 60: 456–463.
[86] Wang Y, Du Z., "A wideband printed dual-antenna system with a novel neutralization line for mobile terminal," IEEE Antennas Wireless Propag Lett. 2013; 12: 1428–1431.
[87] S.-W. Su, et al., "Printed MIMO-antenna system using neutralization-line technique for wireless USB-dongle applications," IEEE Trans. Antennas Propag., vol. 60, no. 2, pp. 456-463, Feb. 2012.
[88] S. Wang and Z. Du, "Decoupled dual-antenna system using crossed neutralization lines for LTE/WWAN smartphone applications," IEEE Antennas Wireless Propag. Lett., vol. 14, pp. 523-526, 2015.
[89] W. A. E. Ali and A. A. Ibrahim, "A compact double-sided MIMO antenna with an improved isolation for UWB applications," AEU-Int. J. Electron. Commun., vol. 82, pp. 7-13, Dec. 2017.
[90] Lim J, et al., "Simultaneous frequency and isolation reconfigurable MIMO PIFA using PIN diodes," IEEE Trans Antenna Propag. 2012; 60: 5939–5945.
[91] Piazza D, et al., "Design and evaluation of a reconfigurable antenna array for MIMO systems," IEEE Trans Antenna Propag. 2008; 56:869–880.
[92] D. E. Anagnostou, et al., "Reconfigurable UWB antenna with RF-MEMS for on demand WLAN rejection," IEEE Trans. Antennas Propag., vol. 62, no. 2, pp. 602-608, Feb. 2014.
[93] S. Soltani, et al., "A port and frequency reconfigurable MIMO slot antenna for WLAN applications," IEEE Trans. Antennas Propag., vol. 64, no. 4, pp. 1209-1217, Apr. 2016.
[94] R. Hussain, et al., "An integrated four-element slot-based MIMO and a UWB sensing antenna system for CR platforms," IEEE Trans. Antennas Propag., vol. 66, no. 2, pp. 978-983, Feb. 2018.
[95] R. Hussain, et al., "4-element concentric pentagonal slot-line-based ultra-wide tuning frequency reconfigurable MIMO antenna system," IEEE Trans. Antennas Propag., vol. 66, no. 8, pp. 4282-4287, Aug. 2018.
[96] J.-H. Lim, et al., ``Simultaneous frequency and isolation reconfigurable MIMO PIFA using PIN diodes," IEEE Trans. Antennas Propag., vol. 60, no. 12, pp. 5939_5946, Dec. 2012.
[97] A. N. Kulkarni and S. K. Sharma, "Frequency reconfigurable microstrip loop antenna covering LTE bands with MIMO implementation and wideband microstrip slot antenna all for portable wireless DTV media player," IEEE Trans. Antennas Propag., vol. 61, no. 2, pp. 964-968, Feb. 2013.
[98] A. Dadgarpour, et al., "Mutual Coupling Reduction in Dielectric Resonator Antennas Using Metasurface Shield for 60 GHz MIMO Systems," IEEE Antennas and Wireless Propagation Letters, vol. 16, pp. 477– 480, 2017.
[99] Hitachi's Research & Development. EBG Structure. Accessed: Aug. 13, 2018. [Online]. Available: http://www.hitachi.com/rd/portal/glossary/e/ebg_structure.html
[100] Y. Rahmat-Samii, "Electromagnetic band gap (EBG) structures in antenna engineering: From fundamentals to recent advances," Proc. Asia_Paci_c Microw. Conf., 2008, pp. 1_2.
[101] M. S. Alam, et al., "Development of electromagnetic band gap structures in the perspective of microstrip antenna design," Int. J. Antennas Propag., vol. 2013, Mar. 2013, Art. no. 507158.
[102] A. Suntives and R. Abhari, "Miniaturization and isolation improvement of a multiple-patch antenna system using electromagnetic bandgap structures," Microw. Opt. Technol. Lett., vol. 55, no. 7, pp. 1609-1612, 2013.
[103] S. Ghosh, et al., "Dual-layer EBG-based miniaturized multi-element antenna for MIMO systems," IEEE Trans. Antennas Propag., vol. 62, no. 8, pp. 3985-3997, Aug. 2014.
[104] B. Mohamadzade and M. Afsahi, "Mutual coupling reduction and gain enhancement in patch array antenna using a planar compact electromagnetic bandgap structure," IET Microw., Antennas Propag., vol. 11, no. 12, pp. 1719-1725, 2017.
[105] J.-Y. Lee, et al., "Reduction of mutual coupling in planar multiple antenna by using 1-D EBG and SRR structures," IEEE Trans. Antennas Propag., vol. 63, no. 9, pp. 4194-4198, Sep. 2015.
[106] Khan MS, et al., "Isolation enhancement of a wideband MIMO antenna using floating parasitic elements," Microwave Opt. Technol. Lett. 2015; 57: 1677–1682.
[107] Huang H, et al., "Broadband omnidirectional dual polarized antenna with high isolation," Microwave Opt. Technol. Lett. 2015; 57: 1848–1852.
[108] Wong K, et al., "Three-antenna MIMO system for WLAN operation in a PDA phone," Microwave Opt. Technol. Lett. 2006; 48: 1238–1242.
[109] Malviya L, et al., "A multi-standard, wide-band 2x2 compact MIMO antenna with ground modification techniques," Int J Microwave Opt. Technol. 2016; 11: 259–267.
[110] H. Bae, et al., "Compact mobile handset MIMO antenna for LTE 700 applications," Microwave Opt. Technol. Lett. 2010; 52: 2419–2422.
[111] S. R. Rengarajan, et al., "Design, analysis, and development of a large KA-band slot array for digital beam-forming application," IEEE Trans. Ant. Propag., AP-57, 10, Oct. 2009, pp. 3103-3109.
[112] J. R. Costa, et al., "Evaluation of a new wideband slot array for MIMO performance enhancement in indoor WLANs," IEEE Trans. Antennas Propag., vol. 59, no. 4, pp. 1200–1206, Apr. 2011.
[113] M. Alibakhshikenari, et al., "A new study to suppress mutual-coupling between waveguide slot array antennas based on metasurface bulkhead for MIMO systems," Asia-Pacific Microwave Conference (APMC), November 6-9, 2018, pp.500-502, Kyoto, Japan.
[114] M. Alibakhshikenari, et al., "New approach to suppress mutual coupling between longitudinal-slotted arrays based on SIW antenna loaded with metal-fences working on VHF/UHF frequency-bands: Study, Investigation, and Principle," Asia-Pacific Microwave Conference (APMC), November 6-9, 2018, pp. 1564-1566, Kyoto, Japan.
[115] M. Alibakhshikenari, et al., "Study on antenna mutual coupling suppression using integrated metasurface isolator for *SAR* and MIMO applications," Proceedings of the 48th European Microwave Conference (EuMC), 25–27 Sept 2018, pp. 1425-1428.
[116] M. Alibakhshikenari, et al., "A new waveguide slot array antenna with high isolation and high antenna bandwidth operation on Ku- and K-bands for radar and MIMO systems", Proceedings of the 48th European Microwave Conference (EuMC), 25–27 Sept 2018, pp. 1421-1424.
[117] M. Alibakhshikenari, et al., "EM Isolation Enhancement Based on Metamaterial Concept in Antenna Array System to Support Full-Duplex Application," 2017 IEEE Asia Pacific Microwave Conference (APMC2017), pp. 740-742, 13-16 Nov 2017, Kuala Lumpur, Malaysia.
[118] M. Alibakhshikenari, et al., "Mutual-Coupling Reduction in Metamaterial SIW Slotted Antenna Arrays Using Metal Fence Isolators for SAR and MIMO Applications", 2018 12th International Congress on Artificial Materials for Novel Wave Phenomena (Metamaterials), Espoo, Finland, 27 August-1 September 2018, Pages: 13 - 15.
[119] M. Alibakhshikenari, et al., "Mutual coupling reduction using metamaterial supersubstrate for high performance & densely packed planar phased arrays," 2018 22nd Int. Microwave and Radar Conference (MIKON), pp. 675 – 678, 14-17 May 2018, Warsaw Univ. of Technology, Poznań, Poland.
[120] M. Alibakhshikenari, et al., "Array antenna for synthetic aperture radar operating in X and Ku-bands: a study to enhance isolation between radiation elements," EUSAR 2018; 12th European Conference on Synthetic Aperture Radar, 4 -7 June, 2018, Aachen, Germany, pp. 1083-1087.
[121] M. Alibakhshikenari, et al., "A technique to suppress mutual coupling in densely packed antenna arrays using metamaterial

supersubstrate," 12th European Conference on Antennas and Propagation (EuCAP 2018), 9-13 April 2018, London, UK.
[122] M. Alibakhshikenari, et al., "mutual coupling suppression between two closely placed microstrip patches using em-bandgap metamaterial fractal loading," IEEE Access, vol. 7, pp. 23606 – 23614, March 5, 2019.
[123] M. Alibakhshikenari, et al., "Study on isolation improvement between closely packed patch antenna arrays based on fractal metamaterial electromagnetic bandgap structures," IET Microwaves, Antennas & Propagation, vol. 12, Issue 14, 28 Nov. 2018, pp. 2241 – 2247.
[124] M. Alibakhshikenari, et al., "Interaction between closely packed array antenna elements using metasurface for applications such as MIMO systems and synthetic aperture radars," Radio Science, vol.53, Issue 11, Nov. 2018, pp. 1368-1381.
[125] M. Alibakhshikenari, et al.,"Mutual-Coupling Isolation Using Embedded Metamaterial EM Bandgap Decoupling Slab for Densely Packed Array Antennas", IEEE Access, vol. 7, pp. 5182 –51840, April 29, 2019.
[126] M. Alibakhshikenari, et al., "High-isolation leaky-wave array antenna based on CRLH metamaterial implemented on SIW with ±30º frequency beam-scanning capability at millimeter-waves", Electronics, 2019, 8, 642, pp. 1-15..
[127] M. Alibakhshikenari, et al., "Meta-surface wall suppression of mutual coupling between microstrip patch antenna arrays for THz-band applications," Progress In Electromagnetics Research Letters, vol. 75, pp.105-111, 2018.
[128] M. Alibakhshikenari, et al., "Antenna mutual coupling suppression over wideband using embedded periphery slot for antenna arrays," Electronics, 2018, 7(9), pp.1-11.
[129] H. Qi, et al., "Mutual coupling suppression between two closely spaced microstrip antennas with an asymmetrical coplanar strip wall," IEEE Antennas Wireless Propag. Lett., vol. 15, pp. 191–194, 2016.
[130] S. Gupta, et al., "Mutual-coupling reduction using metasurface corrugations for 28 GHz MIMO applications," IEEE Antennas Wireless Propag. Lett., vol. 16, pp. 2763–2766, 2017.
[131] R. Karimian, et al., "Low mutual coupling 60-GHz MIMO antenna system with frequency selective surface wall," IEEE Antennas Wireless Propag. Lett., vol. 16, pp. 373–376, 2017.
[132] M. Alibakhshikenari, et al., "Surface wave reduction in antenna arrays using metasurface inclusion for MIMO and SAR systems," Radio Science, Oct. 2019, pp.1067-1075.
[133] M. Alibakhshikenari, et al., "Study on isolation and radiation behaviours of a 34×34 array-antennas based on SIW and metasurface properties for applications in terahertz band over 125-300 GHz," Optik, International Journal for Light and Electron Optics, vol.206, March 2020, 163222.
[134] M. Alibakhshikenari, et al., "Isolation enhancement of densely packed array antennas with periodic MTM-photonic bandgap for SAR and MIMO systems," IET Microwaves, Antennas & Propagation, vol. 14, Issue 3, Feb. 2020, pp. 183 - 188.
[135] Farahani, H.S., et al., "Mutual coupling reduction in patch antenna arrays using a UC-EBG superstrate," IEEE Antennas Wirel. Propag. Lett., Vol. 9, pp. 57–59, 2010.
[136] OuYang, J., et al., "Reduction of mutual coupling of closely spaced microstrip MIMO antennas for WLAN application," IEEE Ant. & Wirel. Propag. Lett., Vol. 10, pp.310-312, 2011.
[137] Yu, A. and X. Zhang: "A novel method to improve the performance of microstrip antenna arrays using a dumbbell EBG structure," IEEE Antennas Wirel. Propag. Lett., vol.2, no. 1, pp.170-172, 2003.
[138] Islam, M. T. and M. S. Alam: "Compact EBG structure for alleviating mutual coupling between patch antenna array elements," Progress in Electromagnetics Research, vol. 137, pp.425-438, 2013.
[139] Zhu, F. G., et al., "Reduction of mutual coupling between closely packed antenna elements using defected ground structure," Electronics Letters, vol. 45, no. 12, pp.601-602, 2012.
[140] Farsi, S., et al., "Mutual coupling reduction of planar antenna by using a simple microstrip u-section," IEEE Ant. and Wirel. Propag. Lett., vol. 11, pp.1501-1503, 2012.
[141] Alsath, M. G., et al., "Implementation of slotted meander line resonators for isolation enhancement in microstrip patch antenna arrays," IEEE Ant. Wireless Propag. Lett., vol. 12, pp.15-18, 2013.
[142] Ghosh. C. K. and S. K. Parui: "Reduction of mutual coupling between E-shaped microstrip antennas by using a simple microstrip I-section," Microwave & Optical Tech. Letters, vol.55, no.11, pp.2544-2549, 2013.
[143] Suwailam, M. M. B., et al., "Mutual coupling reduction between microstrip patch antennas using slotted-complementary split-ring resonators," IEEE Antennas Wireless Propagation Letters, vol. 9, pp.876-878, 2010.
[144] Shafique, M. F., et al., "Coupling suppression in densely packed microstrip arrays using metamaterial structure," Microwave and Optical Technology Letters, vol. 57, no. 3, pp.759-763, 2015.
[145] Yang, X. M., et al., "Reduction of mutual coupling between closely packed patch antenna using waveguide metamaterials," IEEE Ant. & Wirel. Prop. Lett., vol.11, pp.389-391, 2012.
[146] Qamar, Z. and H. C. Park: "Compact waveguided metamaterials for suppression of mutual coupling in microstrip array," Progress in Electromagnetic Research, vol. 149, pp.183-192, 2014.
[147] Jeet Ghosh, et al., "Mutual coupling reduction between closely placed microstrip patch antenna using meander line resonator," Progress in Electromag. Research Lett., vol. 59, pp.115-122, 2016.
[148] Xu Yang, et al., "Isolation enhancement in patch antenna array with fractal UC-EBG structure and cross slot," IEEE Antennas Wireless Propagation Letters, vol. 16, pp. 2175-2178, 2017.
[149] Luyu Zhao, et al., "A high-pass antenna interference cancellation chip for mutual coupling reduction of antennas in contiguous frequency bands," IEEE Access, vol.6, pp. 38097-38105, 2018.
[150] Kai Yu, et al., "Mutual coupling reduction of a MIMO antenna array using 3-D novel meta-material structures," Applied Computational Electromagnetics Society Journal, vol.33, no.7, pp.758-763, 2018.